Adeno-associated virus 2 infection in children with non-A-E hepatitis

Antonia Ho[1]*, Richard Orton[1]*, Rachel Tayler[2]*, Patawee Asamaphan[1]*, Vanessa Herder[1]*, Chris Davis*[1], Lily Tong[1], Katherine Smollett[1], Maria Manali[1], Jay Allan[1], Konrad Rawlik[3], Sarah E. McDonald[1], Elen Vink[1], Louisa Pollock[2], Louise Gannon[4], Clair Evans[5], Jim McMenamin[6], Kirsty Roy[6], Kimberly Marsh[6], Titus Divala[6], Matthew TG Holden[6], Michael Lockhart[6], David Yirrell[6], Sandra Currie[6], Maureen O'Leary[6], David Henderson[6], Samantha J. Shepherd[7], Celia Jackson[7], Rory Gunson[7], Alasdair MacLean[7], Neil McInnes[7], Amanda Bradley-Stewart[8], Richard Battle[9], Jill Hollenbach[10], Paul Henderson[11], Miranda Odam[3], Primrose Chikowore[3], Wilna Oosthuyzen [3], Meera Chand[12], Melissa Shea Hamilton[13], Diego Estrada-Rivadeneyra[13], Michael Levin[13], Nikos Avramidis[3], Erola Pairo-Castineira[3], Veronique Vitart[3,14], Craig Wilkie[15], Surajit Ray[15], DIAMONDS consortium♦, ISARIC4C Investigators♦, Massimo Palmarini[1], David L. Robertson[1†], Ana da Silva Filipe[1†], Brian J. Willett[1†], Judith Breuer[16†], Malcolm G. Semple[17†], David Turner[9†], J Kenneth Baillie[3,13†], Emma C. Thomson[1,18†]

1. Medical Research Council-University of Glasgow Centre for Virus Research, Glasgow, UK
2. Department of Paediatrics, Royal Hospital for Children, Glasgow, UK
3. Pandemic Science Hub, Centre for Inflammation Research and Roslin Institute, University of Edinburgh, Edinburgh, UK
4. Department of Paediatrics, NHS Tayside, UK
5. Department of Pathology, Queen Elizabeth University Hospital, Glasgow, UK
6. Public Health Scotland, Glasgow, UK
7. West of Scotland Specialist Virology Centre, Glasgow, UK
8. Virology Laboratory, Ninewells Hospital, Dundee, UK

9. Histocompatibility and Immunogenetics (H&I) Laboratory, Scottish National Blood Transfusion Service, Edinburgh Royal Infirmary, Edinburgh, UK
10. University of California, San Francisco, USA
11. Department of Child Life and Health, University of Edinburgh, UK
12. UK Health Security Agency, UK
13. Section of Paediatric Infectious Disease, Department of Infectious Disease, Imperial College London, London, UK
14. MRC Human Genetics Unit, Institute for Genetics and Cancer, University of Edinburgh, UK
15. School of Mathematics and Statistics, University of Glasgow, Glasgow, UK
16. University College London, London, UK
17. Pandemic Institute, University of Liverpool, Liverpool, UK
18. Department of Clinical Research, London School of Hygiene and Tropical Medicine, London, UK

*These authors contributed equally to this work

†These authors contributed equally to this work

♦A list of authors and their affiliations appears at the end of the paper.

Summary paragraph

An outbreak of acute hepatitis of unknown aetiology in children was reported in Scotland in April 2022[1] and has now been identified in 35 countries[2]. Several recent studies have suggested an association with human adenovirus (HAdV), a virus not commonly associated with hepatitis. Here we report a detailed case-control investigation and find an association between adeno-associated virus (AAV2) infection and host genetics in disease susceptibility. Using next-generation sequencing (NGS), reverse transcription-polymerase chain reaction (RT-PCR), serology and *in situ* hybridisation (ISH), we detected recent infection with AAV2 in the plasma and liver samples of 26/32 (81%) hepatitis cases versus 5/74 (7%) of controls. Further, AAV2 was detected within ballooned hepatocytes alongside a prominent T cell infiltrate in liver biopsies. In keeping with a CD4+ T-cell-mediated immune pathology, the Human Leucocyte Antigen (HLA) class II DRB1*04:01 allele was identified in 25/27 cases (93%), compared with a background frequency of 10/64 (15.6%; $p=5.49 \times 10^{-12}$). In summary, we report an outbreak of acute paediatric hepatitis associated with AAV2 infection (most likely acquired as a coinfection with HAdV which is required as a "helper virus" to support AAV2 replication) and HLA class II-related disease susceptibility.

Main text

Hepatitis outbreak in Scottish children

In April 2022, several hospitals in Scotland reported that children were presenting to medical practitioners withacute severe hepatitis of unknown aetiology (Fig. 1a)[1]. Elsewhere in the UK, 270 similar presentations were subsequently reported, for which 15 children requireding liver transplantation[3]. The World Health Organisation (WHO) have now registered over 1010 probable cases fulfilling their case definition in 35 countries[2]. Understanding the underlying cause of this new disease is a global public health imperative.

Detailed clinical investigations, carried out as part of the public health response, excluded common causes of acute hepatitis including viral hepatitis, drug toxicity and autoimmune hepatitis. Unexpectedly, as it is not a common cause of hepatitis, recent or active human adenovirus (HAdV) infection was identified in Scotland, England and the USA in a high proportion of cases[4-6]. An increase in HAdV diagnoses in Scotland directly preceded the outbreak of unexplained hepatitis in children of a similar age (Fig. 1a,b). SARS-CoV-2 had been circulating for two years and peaked several months before the rise in hepatitis cases (Fig. 1c)[3]. Human herpesvirus 6 (HHV6A and HHV6B) infections were not detected at higher levels during 2021 or 2022 (Fig. 1d).

Research investigation

To investigate the aetiology of the acute hepatitis cases, we recruited 32 affected children, who presented to hospital between 14 March and 20 August 2022 and met the Public Health Scotland (PHS) case definition criteria for inclusion in the International Severe Acute Respiratory and Emerging Infections Consortium (ISARIC) WHO Clinical Characterisation Protocol UK (CCP-UK) [ISRCTN 66726260][7]. Control samples were obtained from the

Diagnosis and Management of Febrile Illness using RNA Personalised Molecular Signature Diagnosis study cohort (DIAMONDS) and from the NHS Greater Glasgow & Clyde (GG&C) Biorepository, under appropriate ethical approvals (**Methods**)

Clinical presentation

The median age of affected patients was 4.1 years (interquartile range (IQR), 2.7 to 5.5 years) (Table 1). Twenty-one of the 32 (66%) children were female, and all were of white ethnicity. Eighteen (56%) of the children reported a subacute history 2-12 weeks prior to acute hepatitis, characterised by an initial gastroenteritis-like illness followed by intermittent vomiting, abdominal pain and fatigue. The majority (23/32) had no other medical conditions: one child had previously received a liver transplant; none of the other cases were immunocompromised and none had received COVID-19 vaccination. All routine blood tests for viral hepatitis, including hepatitis A, B, C, E, acute Epstein-Barr virus (EBV), cytomegalovirus (CMV), human herpes virus (HHV) 6/7 and herpes simplex virus (HSV) were negative (Supplementary Table 1). Four cases had low titre (1:80) anti-nuclear antibodies (ANA), and 3 cases low titre (1:40) anti-smooth muscle antibodies (ASMA) but other markers of autoimmunity were negative (Table 1; Supplementary Table 2).

Following hospitalisation, liver biopsies were obtained from five children and revealed evidence of lobular hepatitis with periportal and interface inflammation, intracellular inclusions, bile duct proliferation and ballooning of hepatocytes of varying severity(Fig. 1e-t). Mild to moderate fibrotic changes were noted with no evidence of confluent fibrosis, and there was an inflammatory infiltrate including Major Histocompatibility Complex (MHC) class II-expressing cells. Modified hepatic activity index scores (Ishak)[8,9] ranged from 6 to 11 (Extended Data Table 1) and the biopsies stained negative for complement.

Four cases required transfer to a specialist liver unit due to significant synthetic liver dysfunction. Two of these were treated with steroid therapy and improved. One received supportive care only and improved spontaneously. The fourth severe case required liver transplantation and was treated with cidofovir for HAdV viraemia and steroids post-transplant. The remaining 28 patients received supportive care only with no antiviral or steroid treatment and all showed gradual resolution of hepatitis over 2-3 months. There were no deaths. The median duration of hospital stay was 6 days (range 1-68 days) (Table 1). In the patients with weakly positive autoantibodies, all had normal or normalising transaminases at last follow up in the absence of anti-inflammatory or immunosuppressive treatment.

Pathogen detection by sequencing

As the epidemiology was in keeping with the emergence of an infectious pathogen, we undertook metagenomic and target enrichment (TE) next generation sequencing (NGS) on all available clinical samples from the first nine recruited patients, including plasma (n=9), liver biopsies (n=4), throat swabs (n=6), faecal samples (n=7) and a rectal swab (n=1), with an average of 14 million sequence reads per sample (Fig. 2a-d; Extended dataset 1). These were obtained between 7-80 days after initial symptom onset. Control subjects were restricted to children recruited in the UK between January 2020 and April 2022. Two comparison groups were identified: Group 1, serum or plasma from 13 age-matched healthy children (10 male, 3 female; age range 3-5 years) and Group 2, serum or plasma from 12 children (8 male, 4 female; age range 1-4 years) with PCR-confirmed HAdV infection and normal transaminases (n=12). The Group 2 controls had been diagnosed by nasopharyngeal aspirate (n=10), by nose swab (n=1) and by stool (n=1) as part of routine clinical investigation and half had

required critical care. There was no significant difference in age between hepatitis cases and Group 1 healthy controls, but some control samples were sampled earlier than case samples (January 2020-April 2022 versus March-April 2022) (Extended Data Table 2a). Group 2 controls were younger (median age 1.4 years; interquartile range (IQR) 1.1-3.1 years, $p<0.001$) and were collected between May 2020 and December 2021 (Extended Data Table 2b). Metagenomic NGS was carried out using protocols designed to identify both RNA and DNA viruses. Semi-agnostic TE sequencing was also performed using VirCapSeq-VERT Capture probes that target the genomes of 207 viral taxa known to infect vertebrates.

TE sequencing reflected metagenomic NGS results but with higher sensitivity and correlated with viral load measured by qRT-PCR (Supplementary Fig.s 1,2**)**. By both methods, the viral genome detected most frequently in affected patient plasma was adeno-associated virus 2 (AAV2) in 9/9 cases (Fig. 2a; Supplementary Table 3; Extended Data Fig. 1). AAV2 was also detected in 4/4 liver biopsies, and in 1/7 faecal, 1/1 rectal and 1/6 throat swab samples. At lower read counts, HAdV-F41 or HAdV-C were detected in 6/9 patients, while HHV6B was detected in 3/4 plasma samples (Extended Data Fig. 1; Supplementary Tables 4, 5; Supplementary Fig. 3). HAdV types C1, 2, 5 and 6 could not be reliably distinguished due to low read counts. The remaining clinical samples were excluded from analysis for HHV by sequencing because murine herpesvirus 1 (MHV1) had been added as an extraction control during routine clinical investigation.

Read counts of AAV2 by TE were high (median 4478 reads/million; IQR 774-10,498 reads/million) in all 9/9 hepatitis cases versus 0/13 Group 1 healthy controls (IQR 0-0 reads/million; $p<0.001$) and 0/12 Group 2 controls (HAdV-infected children with normal LFTs; IQR 0-0 reads/million; $p<0.001$) (Supplementary Table 5). HAdV reads were detected in 6/12 Group 2 HAdV-positive controls (median 0.82 reads/million, IQR 0-1053

reads/million) despite plasma/sera being a suboptimal sample type to detect HAdV, and in 3/9 cases (median 0 reads/million; IQR 0-0.6 reads/million), more than in 0/13 Group 1 healthy controls (IQR 0-0 reads/million; p=0.055). HHV6B was also detected in 3/4 hepatitis cases versus 0/13 healthy controls (median 1.9 reads/million, IQR 0.3-3.5 reads/million and IQR 0-0 reads/million; p=0.006, respectively) (Supplementary Table 4). However, HHV6B read counts did not differ significantly between hepatitis cases and Group 2 controls (median 0; IQR 0-0.04 reads per million; p=0.16), in keeping with reactivation of HHV6B in the context of severe illness. While metagenomic and TE sequencing from the 13 age-matched healthy control samples (Group 1) revealed no evidence of AAV2, HAdV or HHV6B in plasma, low read counts of EBV, CMV and HHV6A were detected in a small number of samples (Supplementary Table 4). In Group 2 (HAdV infection and normal LFTs), herpesviruses were detected in 9/12 samples, including 2/12 (as described above) with detectable numbers of HHV6B reads (1050 and 5062 reads/million respectively), confirmed by PCR.

Sequence and phylogenetic analysis

Near-full genomes of AAV2 were obtained from all 9 affected patients (accession numbers OP019741-OP019749) and in all cases, two large open reading frames corresponding to the *rep* and *cap* genes, flanked by ITR regions, were identified. Seven distinct sequences of AAV2 were noted (Extended Data Fig. 2), forming a single clade with 4 AAV2 genomes detected in France between 2004 and 2015. Two of three identical sequences were known to have come from the same household so are almost certainly linked epidemiologically, while the third occurred around the same time but was not known to be linked to the other cases. Sequences from the liver matched those detected in plasma. Several mutations within the VP1-3 genes were noted to be over-represented in the sequences derived from patients with

hepatitis when compared with reference sequences (Extended Data Fig. 2). Notably, 9 of the capsid gene mutations over-represented in hepatitis cases (V151A, R447K, T450A, Q457M, S492A, E499D, F533Y, R585S and R588T) are associated with an AAV2 variant that has an altered phenotype, including substantial evasion of neutralising antibodies directed against wild-type AAV2, enhanced production yields, reduced heparin binding, increased virion stability and more localised spread in a mouse model[10 8 9].

A full genome of HAdV-F41 was obtained from a faecal sample (accession number OP019750) and was found to be closest phylogenetically to two genomes reported from Germany in 2019 and 2022 (Extended Data Fig. 2). Contigs matching to other human pathogens, including human coronavirus NL63, rhinovirus C, enterovirus B, human parainfluenza virus 2 and 3, norovirus, and both beta- and gammaherpesviruses were also detected across cases, albeit not consistently. These findings were confirmed by PCR (Supplementary Table 1).

Confirmatory PCR testing of cases 1-9

PCR testing for AAV2 was positive in all 9 cases. Standards were used to estimate viral load of positive samples (Supplementary Fig. 2). All 9 plasma samples tested negative by PCR for HHV6, HSV, CMV and EBV. Two of the four liver biopsy specimens tested positive for HHV6 (cycle threshold (Ct) 33 and 36) (Supplementary Table 1). HAdV was detected in 3/9 plasma samples, 3/4 liver biopsies, 2/6 throat swabs, 4/7 faecal samples and 1/1 rectal swab. The lower detection of HAdV and HHV6 by PCR compared to enrichment sequencing likely reflects a slightly lower sensitivity of the PCR assay. The low numbers of HAdV-positive samples detected using both assays may reflect plasma being a suboptimal sample type for HAdV detection (whole blood samples were unavailable).

Case control study

To investigate the presence of AAV2 and the candidate helper viruses HAdV and HHV6B in plasma samples from the hepatitis cases, we undertook a case-control study, comparing 32 hepatitis cases with the Group 1 and 2 controls described above, and two additional control groups (Fig. 2a-f). Group 3 controls, 33 children (18 males and 15 females aged 2-16 years) with raised transaminases who were HAdV PCR negative, were used to test the hypothesis that reactivation of AAV2 may occur in children with severe hepatitis and may be a correlate of liver dysfunction. These children were older (median age 10.2 years; IQR 7-13.6 years, $p<0.001$) than the study cases (Extended Data Table 2b) and 15/33 had required critical care for ventilatory or cardiovascular support. Group 4 controls, residual plasma/serum from 16 Scottish children aged 10 and under attending hospital contemporaneously with the hepatitis cases between March and April 2022, were used to determine whether AAV2 was circulating widely in children in healthcare facilities across Scotland at the time the hepatitis cases were admitted to hospital. Clinical details, including liver function were not available in this group. To ensure the quantification of the AAV2 was performed accurately, we confirmed standard curve concentrations using droplet digital PCR (ddPCR; Methods).

Significance differences between groups for viral loads in plasma were calculated using the Mann-Whitney test (two-tailed). AAV2 qRT-PCR of plasma from 26/32 cases was positive with a median estimated copy number of 66,100 copies/ml (IQR 13,461- 300,277 copies/ml), higher than all control groups ($p<0.001$ for all case-control comparisons). The median copy number in control Groups 1-3 was below the detection limit. A median of 3,268 copies/ml, (detection threshold of 3,200 copies/ml) was present in control Group 4 suggesting that AAV2 was circulating at low level in children during March and April 2022 (Fig. 2c;

Extended dataset 2). Although five plasma samples from hepatitis cases were HAdV-positive by PCR, and one tested positive by PCR for HHV6 DNA, these results were not significantly more common than in control samples (Supplementary Fig. 3).

Next, five liver biopsies from hepatitis cases were compared with 19 control residual liver biopsies from children under 18 years old. The median AAV2 viral load was 3,721,497 copies/mm^3 of liver (IQR 3,308,243 -6,717,616 copies/ mm^3) in hepatitis cases, and 64 copies/mm^3 of liver (IQR 20-83 copies/mm^3) in controls; $p<0.001$ (Fig. 2d; Extended dataset 3). Glyceraldehyde-3-phosphate dehydrogenase (GAPDH) was used as a marker of extraction efficiency in all samples and was similar in case and control samples. When outliers were removed, statistical significance was retained (Supplementary Fig. 4).

Longitudinal sampling

To investigate AAV2 viraemia and liver function over time, longitudinal PCR testing was performed in 14 cases from whom multiple retrospective plasma samples were available (Extended Data Fig. 3). Spearman's rank correlation coefficients for the relationships between the trajectories of viral load and ALT and bilirubin were positive for most cases. However, overall statistical significance could not be confirmed due to sample size.

Where samples were available, we screened for the presence of AAV2-specific IgM and IgG within patient samples and Groups 1 and 4 healthy and contemporaneous controls (Fig. 2e,f; Supplementary Fig. 5; Extended dataset 4). Anti-AAV2 IgM was detected in 15/23 (65.2%) of hepatitis cases, but only 1/13 Group 1 healthy control samples (7.7%) and 2/16 (12.5%) Group 4 Scottish contemporaneous controls, respectively. For the case samples that tested negative for AAV2-specific IgM, four patients were noted to be fewer than three days post-

onset of illness and two patients were more than 77 days post-illness onset. IgG was detected in 21/23 (91.3%) of cases, in 8/13 (61.5%) of age-matched healthy controls and in 9/16 (56.3%) of Scottish healthy controls. Of the two seronegative patients, both were early time points, likely sampled prior to expected seroconversion (less than 3 days after the onset of illness).

SARS-CoV-2 infection

Routine clinical investigation detected SARS-CoV-2 nucleic acid in nasopharyngeal samples from only 3/31 (9.6%) children at the time of illness, two of whom were also seropositive. The third became infected after the onset of hepatitis. SARS-CoV-2 was not detected by PCR or by sequencing in any of the case or control samples available for analysis, including liver samples. Nevertheless, to investigate the possibility that unexplained hepatitis in children might relate to a prior infection with SARS-CoV-2 or other seasonal coronaviruses, we carried out serological analysis of 23 available residual samples from cases. IgG antibody titres were measured quantitatively against SARS-CoV-2 spike (S) protein, N-terminal domain (NTD) and receptor binding domain (RBD) of spike, and nucleocapsid (N), and the human seasonal coronaviruses (HCoVs) 229E, OC43, NL63 and HKU1. Electrochemiluminescence assay (MSD-ECL) for coronavirus-specific IgG revealed prior exposure to seasonal coronaviruses; with strong responses detected against NL63 (17/23) and OC43 (21/23) (Extended Data Fig. 4a). In comparison, plasma from 12/23 children displayed high reactivity against HKU1 while only 3/23 reacted strongly against 229E. Plasma from eleven children reacted with two or more SARS-CoV-2 antigens; N, S, NTD or RBD. A single additional child reacted solely with N, indicating that in total, 12/23 displayed serological evidence of prior exposure to SARS-CoV-2 (Extended Data Fig. 4b). In summary, 12/23 (52%) of the children displayed evidence of prior exposure to SARS-CoV-2;

a lower level than SARS-CoV-2 seroprevalence in children aged 5-11 years in Scotland between 14th March and 27th June 2022 (when PHS enhanced surveillance for COVID-19 was discontinued), reported as between 59.0% (95% CI 50.6-71.2) and 72.4% (53.9-78.8)[10], indicating no direct link between COVID-19 and the outbreak of acute hepatitis.

Host genetics and HLA typing

To investigate whether some children might be genetically more susceptible to non-A-E hepatitis, 27 cases and 64 Scottish platelet apheresis donor local controls were genotyped using high resolution typing for all HLA loci (HLA-A, B, C, DRB1, DRB3/4/5, DQA1, DQB1, DPA1 and DPB1) (Extended Dataset 5). 25/27 (92.6%) of affected patients were positive for at least one copy of the DRB1*04:01 allele versus 10/64 (15.6%) of controls; allele frequency in patients was 0.54 versus 0.08 in controls (OR 13.7 (95% CI 5.5-35.1), $p= 5.49 \times 10^{-12}$). The frequency of the DRB1*04:01 allele (based on imputation of HLA alleles) in a control set of unrelated UK Biobank participants (n=29,379) was found to be 0.11 (2,942/29,379 allele carriers, OR 112.3 (95% CI 26.6 – 474.5), $p=3.27 \times 10^{-23}$) and in British/Irish North-West European (BINWE) individuals on the Anthony Nolan charity register, the allele frequency of DRB1*04:01 is also 0.11[10]. To check for cryptic relatedness among patients and population stratification, we performed genome-wide microarray genotyping in 19 cases and excluded participants with a conservative relatedness threshold (identity-by-state >0.4). Comparing to well-matched participants in the UK Biobank (Extended Data Fig. 5**)**, similar signals for association with disease by allele frequency ($p=8.96 \times 10^{-6}$) and across the three possible biallelic genotypes at this locus ($p=1.2 \times 10^{-9}$) were obtained.

In addition to the DRB1 association, 23/27 patients were positive for DQA1*03:03 versus 11/64 controls (allele frequency 0.54 vs 0.09, odds ratio (OR) 12.3 (5.1-30.7), $p = 1.9 \times 10^{-11}$) and 26/27 patients were positive for DRB4*01:03 versus 21/64 controls (allele frequency 0.67 vs 0.17 OR 9.4 (4.4-21.3), $p = 1.8 \times 10^{-10}$). Due to strong linkage disequilibrium in this region of the genome, it is not possible to be certain which is the causal susceptibility allele.

In situ hybridisation and immune typing

To investigate the presence of AAV2, HAdV and HHV6 in liver biopsies, we carried out *in situ* hybridisation (ISH). Liver biopsies of all patients were characterised by AAV2 RNA within the nuclei and cytoplasm of "ballooned" hepatocytes and in arterial endothelial cells indicating the presence of replicating virus (Fig. 3a-h). AAV2 positive cells were quantified at high level in all cases using QuPath in biopsies of 5 non-A-non-E hepatitis, ranging from 1.2 to 4.7%. This level is similar to that seen in hepatitis associated with other viruses[11,12]. Consistent with low levels of HHV6B and HAdV sequence reads present in the case biopsies, negligible levels of viral RNA from these viruses were detected by ISH.

To investigate the possibility of an immune-mediated pathogenesis of disease in the liver, multiplex analysis of liver samples was carried out using CO-Detection by indEXing (CODEX) for a variety of immune cellular markers including CD3, CD4, CD8, PD-L1, CD107a, CD20, CD31, CD44, CD68, Mx1 and PanCK (Fig. 4a-d; Supplementary Fig. 6,7). In the explant liver of patient CVR35, prominent disordered proliferation of epithelial cells throughout the liver tissue was evident, with increased CD68+ macrophages, activated CD4+ and CD8+ T cells, as well as CD20+ B cells. High expression of the interferon-induced GTP-binding protein Mx-1 was also noted, indicating activation of the innate immune response[13].

Conclusions/final statements

In this study, we report the association of AAV2 and the class II HLA allele DRB1*04:01 with an outbreak of paediatric non-A-E hepatitis, virus being detected independently by sequencing, real-time PCR and *in situ* hybridisation. Liver tissue from biopsies of all patients was characterised by AAV2 RNA (indicating replicating virus) within the nucleus and cytoplasm of "ballooned" hepatocytes and by a dense CD4+ and CD8+ infiltrate in the liver with an activated phenotype. A CD4+ T-helper cell-mediated immunopathological response triggered by exposure to AAV2 infection is highly likely, consistent with the markedly increased frequency of the MHC class II DRB1*04:01 allele in affected children.

AAV2 is a small non-enveloped virus with a single-stranded DNA genome of around 4,675 nucleotides in length belonging to the species adeno-associated dependoparvovirus A (genus Dependoparvovirus, family Parvoviridae).[14] It was first described in 1965 and infects up to 80% of the adult population. Seroconversion occurs in early childhood following respiratory infection[15]. In a prospective study in the USA, the earliest seroconversion to AAV2 infection occurred in a 9-month-old child and its seroprevalence increased from 24.2% to 38.7% in 3 and 5-year-old children, respectively[16]. This age range coincides with that of the cases in this study, suggesting that illness may be related to primary infection with AAV2 rather than its reactivation. In line with this hypothesis, we demonstrated anti-AAV2 IgM reactivity in the majority of affected children. AAV2 relies on coinfection with a helper virus for replication, most commonly HAdV or a herpesvirus. Most clinical samples taken at presentation with hepatitis were obtained more than 20 days after initial symptom onset, which could explain the absence of a helper virus in some samples, and low viral loads in positive samples. In an exploratory study using NGS, we detected two candidate helper viruses at low level in the hepatitis cases: HAdV and HHV6B (6/9 and 3/9 cases respectively). These viruses were not confirmed to be higher in cases than controls in plasma or liver samples in our larger case-

control study; HHV6B was also present in two control groups that included children with severe HAdV infection and children with hepatitis of alternative aetiology. As HHV-6 can establish latency and can integrate its genome into the human chromosome, it may reactivate following concomitant illness (or immunosuppression) and may represent either an opportunistic bystander or a pathogen.

We hypothesise that AAV2 is directly implicated in the pathology of the 2022 outbreak of non-A-E hepatitis in children, following transmission as a co-infection with HAdV or less likely due to reactivation following HAdV or HHV6 infection. Our results also support an association between an HLA class II haplotype and disease susceptibility. A CD4+ T-cell-mediated response may direct a maladaptive T cytotoxic or B cell-mediated immunopathology. In support of this, a CD8+ cell-mediated response directed against the AAV2 viral capsid (VP1) in association with hepatitis was reported in early trials of AAV2 when used as a vector for gene therapy[17-19]. Hepatitis remains a common phenomenon in AAV-vectored gene therapy, usually treated pre-emptively with steroids before and for several weeks after treatment, and in rare cases has been associated with deaths from fulminant hepatic failure[20,21]. As a result of this investigation, further studies to investigate HLA association with severe illness in gene therapy recipients are indicated. Importantly, we did not find features of autoimmune hepatitis (AIH) in affected children, by serology or histology. In a recent cohort of Scottish children with AIH, the majority had evidence of seropositive disease (100% of patients with type II AIH tested positive for anti-LKM1). Further, AIH patients were older in age (median age 11.4yrs vs. 4.1yrs in our cohort) and had significantly lower median ALT at diagnosis (444 IU/L versus 1756 IU/L). None improved without treatment.[22]

An alternative explanation is that AAV2 is not directly involved in pathology and is rather a biomarker of infection with HAdV. Over half of our cases had subacute symptoms, with a median onset of 42 days before the onset of jaundice. The opportunity to detect virus by sequencing was therefore reduced, as samples were collected after this stage of illness. Further, whole blood samples would have been likely to increase the sensitivity of detection, but only serum/plasma samples were available. We consider this alternative hypothesis to be less likely because we did not detect AAV2 in a control group of children with HAdV infection who had normal liver function. However, HAdV41 is a common cause of diarrhoea in young children[23] and co-infection of AAV2 with HAdV41 may explain early gastrointestinal symptoms in affected children. In contrast, although adenovirus-associated hepatitis has been described, particularly among immunocompromised individuals,[24] HAdV41 has not previously been associated with severe hepatitis. In the recent outbreaks of unexplained hepatitis in children, it has been associated inconsistently[4-6,25-27].

We also investigated the possibility that unexplained cases of hepatitis were linked to prior COVID-19 infection. Direct SARS-CoV-2 liver injury is unlikely, since few of our hepatitis cases (3 of 31) were SARS-CoV-2 PCR-positive on admission, and we did not identify SARS-CoV-2 by PCR or sequencing in any of the clinical samples from cases, including liver biopsies. Further, the SARS-CoV-2 seroprevalence in hepatitis cases was lower than community cases at that time.[3] This is in keeping with a case-control analysis by UKHSA that found no difference in SARS-CoV-2 PCR positivity between hepatitis cases and children presenting to emergency departments between January and June 2022.[3] Nevertheless, we cannot at this time fully exclude a post-COVID-19 immune-mediated phenomenon, for example a link to HLA class II type, in susceptible children.

There are several limitations to this study. Firstly, the presence of AAV2 in hepatitis cases but not Group 1-3 controls may have arisen due to seasonal variation in AAV2 transmission, as some controls were sampled earlier than cases. We included a contemporaneous control group (Group 4) to address this possibility. Low viral loads of AAV2 were detected in a small number of Group 4 control subjects in keeping with the presence of the circulating virus in children at the time the cases occurred. Secondly, the presence of AAV2 in cases is an association and may not represent direct aetiology; rather the AAV2 may be a useful biomarker of recent HAdV (or less likely HHV6B) infection. We do not consider it likely that AAV2 simply represents a marker of liver damage because it was not present in cases of severe hepatitis of alternative aetiology and significantly, we detected AAV2 in ballooned hepatocytes by ISH. The strong association of the HLA-DRB1*04:01 allele, known to be associated with autoimmune[28] and extra-articular manifestations of rheumatoid arthritis[29] supports a strong host genetic impact on susceptibility. This analysis is affected by strong linkage disequilibrium and larger studies are required to confirm the definitive allele association. The HLA association and the presence of an activated T cell infiltrate alongside AAV2-infected cells in the liver is in keeping with a CD4+-mediated immune pathology[30]. We consider autoimmune disease to be less likely due to the absence of autoantibodies in affected cases and the absence of typical histology in liver specimens. It is also plausible that simultaneous HAdV infection, with a coinfecting or reactivated AAV2 infection has resulted, for a proportion of children who are more susceptible (due to the HLA class II allele HLA-DRB1*04:01), in a more severe outcome than might normally be expected for these commonly circulating viruses. Peptide mapping experiments are indicated in future studies to investigate the nature of the HLA class II-restricted T cell response.

The 2022 outbreak of AAV-2 associated paediatric hepatitis that we describe in this study may have arisen because of changes in exposure patterns to AAV2, HAdV and HHV6B as an indirect consequence of the COVID-19 pandemic. The circulation of common human viruses was interrupted in 2020 by the implementation of non-pharmaceutical interventions, including physical distancing and travel restrictions, instituted to mitigate SARS-CoV-2 transmission. Once restrictions were lifted, genetically susceptible children may have had a higher chance of being co-exposed to HAdV and AAV2 for the first time, creating a synchronised wave of severe disease. Larger case-control studies are urgently needed to confirm the role of AAV2 and HLA in the aetiology of unexplained non-A-E paediatric hepatitis. Retrospective testing of samples from sporadic cases of unexplained hepatitis in children is also needed.

443 **Table 1. Demographic and clinical characteristics of the 32 cases with unexplained**

444 **hepatitis.**

Demographics	
Age (years)[a]	4.1 (2.7-5.5, 0.9-10.6) years
Sex - female[b]	20 (63%)
Co-morbidity[b]	9 (28%)[c]
Biochemistry	
Peak bilirubin[a] (µmol/l)	82 (36-160, 3-387)
Peak ALT[a] (U/L)	1757 (708-2763, 333-5417)
Peak AST[a] (U/L)	2048 (833-3408, 424-6908)
Peak GGT[a] (U/L)	124 (91-162, 18-720)
Peak INR[a]	1.2 (1.1-1.4, 1.0-2.9)
Peak CRP[a] (mg/L)	5 (3-11, 1-117)
Caeruloplasmin[a] (n=24) (g/L)	0.36 (0.33-0.39, 0.22-0.52)
Key autoimmune parameters	
IgG[a] (g/L)	11.8 (9.9-14.3, 1.5-21.0)
Coeliac screen (TTG antibody) (n=26)	26 normal range
Anti-mitochondrial antibody	32 negative
Anti-smooth muscle antibody (SMA)	29 negative, 3 low positive (1:40)[c]
Anti-liver kidney microsomal (LKM) 1 antibody	32 negative
Anti-nuclear antibody (ANA)	28 negative, 4 weak positive 1:80 titre[c]
Clinical presentation	
Symptoms at presentation[b] • Vomiting • Jaundice • Poor appetite • Lethargy/fatigue • Abdominal pain • Diarrhoea	 22 (69%) 21 (66%) 12 (38%) 10 (31%) 10 (31%) 4 (13%)
Sub-acute symptoms for ≥14 days prior to presentation (n=32)	18 (56%)
Sub-acute symptoms reported (n=18) • Intermittent vomiting • Initial gastroenteritis-like illness • Abdominal pain • Lethargy/fatigue • Poor appetite • Weight loss	 15 (83%) 12 (67%) 9 (50%) 7 (39%) 6 (33%) 6 (33%)
Approximate duration of sub-acute symptoms prior to presentation[ad]	42 (27-52, 14-85) days
Length of hospital stay[ae]	6 (4-10, 1-68) days
Required transfer to tertiary liver unit	4 (12.5%)

Required liver transplant	1 (3%)

a. Median (interquartile range, range); b. number (%) denominator=32 unless otherwise specified. c. See Supplementary Data for additional clinical details. d. n=16 patients with data available e. n=30, one patient long-term inpatient for unrelated condition, one patient identifed and managed as outpatient.

Figure Legends

Fig. 1: Epidemiology and histological appearance of paediatric hepatitis cases in Scottish children. a, The emergence of acute non-A to E hepatitis in children March-September 2022 [3], **b**, Cases of HAdV , **c**, SARS-CoV-2 and **d,** HHV6 in children aged ≤10 years in Scotland January 2019 to September 2022. Diagnoses in children aged ≤5 years are shown in black and 6-10 years in grey. **e-t,** Histopathology of non-A-E hepatitis cases. **e, i, m, q,** Serial sections of formalin-fixed and paraffin-embedded (FFPE) liver tissue sections (one section for each stain per subject) stained with haematoxylin and eosin (H&E) , **f, j, n, r,** reticulin (highlighting structural organisation , and **g, k, o, s** Masson (highlighting collagen fibres). **m-p**, The regular lobular structure of the control healthy liver (145783) is not recognisable in **e-h,** sections collected from CVR35 who was transplanted. **h,** Immunohistochemistry shows an increase of $MHCII^+$ cells in tissues from CVR35 compared to **l, t,** control liver (bars in **e-h** and **m-p** = 400 μm). **i-l,** higher magnifications micrographs of panels **e-l** showing details of liver histopathology. **i,** In CVR35, enlarged (ballooned) and vacuolated hepatocytes (*) are evident compared to hepatocytes with a regular morphology from q**,** control liver (145783; arrow) with a regular sinus (+). **j**, In CVR35,) the reticulin staining shows destruction of the sinus structures and irregularly arranged fibres, while **r,** control liver shows fibres lining the sinus. **k,** In CVR35, Masson staining shows an increase of collagen fibres (in blue; *) as opposed to minimal staining of fibres (arrow) in a **s,** control liver. **l,** High magnification showing accumulation of $MHCII^+$ cells in the liver (*) of CVR35 while in **t,** control liver , staining is limited to Kupffer cells (bars in **i-Pp** = 50 μm).

Fig. 2: AAV2 detection in paediatric hepatitis cases. a, Heatmap of HAdV and AAV2 reads detected in hepatitis cases by target enrichment sequencing. Samples obtained for routine clinical investigation (plasma, liver, faeces, rectal and throat swab) were

retrospectively sequenced following DNA or RNA extraction. AAV2 read counts are shown from 0 to >100 reads/million in green (upper row) and HAdV read counts are shown from 0 to >10 reads/million in red (lower row). **b,** Heatmap of viral reads from plasma in hepatitis cases and plasma/sera from controls. Plasma samples from hepatitis cases, and plasma or sera samples from children with HAdV infection and age-matched healthy controls were sequenced following DNA or RNA extraction. AAV2 read counts are shown from 0 to >50 reads/million in green and HAdV read counts are shown from 0 to >5 reads/million in red. The number of days between initial symptom onset and sample are indicated. **c,** AAV2 real-time qRT-PCR of serum/plasma in 32 hepatitis cases versus 74 control subjects in four groups (13 in Group 1, 12 in Group 2, 33 in Group 3 and 16 in Group 4). The detection threshold of the assay (3200 copies/ml) is shown as a dotted line. Values are shown as a scatter plot with a median line. Statistical analysis was performed using the Mann-Whitney test (two-tailed). **d,** AAV2 real-time qRT-PCR of liver biopsies in 5 hepatitis cases versus 19 controls. Statistical analysis was performed using the Mann Whitney test (two-tailed). **e,** IgM responses determined by ELISA in 22 hepatitis cases versus 29 controls (13 in Group 3, 16 in Group 4)**f,** IgG responses determined by ELISA in 22 hepatitis cases versus 29 controls (13 in Group 3, 16 in Group 4). Statistical analysis was performed using the Mann Whitney test (two-tailed). Data in panels c-f were carried out in triplicate.

Fig. 3 *In situ* hybridization of AAV2 in liver tissue. In panels **a-h,** RNA *in situ*-hybridisation for the detection of AAV2 RNA in sections of FFPE liver tissues from children (one section per patient) with non A-E hepatitis is shown. In **a,** AAV-2 RNA (red signal, arrows) is detected in the endothelial cells of arteries in an explant liver section from patient CVR35. The vascular lumen is highlighted with an asterisk (*). Positive AAV2 signal is shown in the nuclei of hepatocytes with vacuolated morphology from patient CVR4 (**b**; arrows) andnegative cell (circle). In **c,** a liver section from patient CVR1 shows AAV2 viral RNA both in the nucleus and in the cytoplasm (bar, 50 μm), while in **d** (CVR9), AAV2 RNA is found only in the nucleus. Panel **e** shows a high percentage of hepatocytes with a positive signal for AAV2 predominantly in the nucleus of hepatocytes (CVR1). AAV2 is not detectable in liver sections from control patients (**f**) in either the endothelial cells or hepatocytes (bar of insert and X, 50 μm). In **g**, inclusion bodies from patient CVR35, left panel, small, dark basophilic intranuclear inclusion bodies in hepatocytes next to the nucleolus (arrows); right panel,bottom right corner, a hepatocyte with a large, pale-basophilic, diffuse intranuclear inclusion body (suggestive of adenovirus infection, arrow) next to a multinucleated giant cell in the liver (*). Bars in **a, b, c, d, f and g** = 50μm; Insets in **c** and **d** = 25μm; **e** = 200μm. AAV2 positive cells were quantified using QuPath (**h**) in biopsies of 5 non-A-non-E hepatitis and control patients; patient CVR35 (transplanted) highlighted in red. Using the entire section, cells were segmented to identify the nuclei and cytoplasm, the algorithm was tuned to detect red signa. All samples were analysed using the same algorithm.

Fig. 4 CO-Detection by indEXing (CODEX) analysis of liver tissue. Liver tissue from CVR35 and a control liver sample show differences in the control (a and c) and the patient

(CVR35; b and d) in cellular composition (c, d); bile ducts (*). Regular structured bile ducts in a control liver biopsy (**a**) arehighlighted by * and green staining of epithelial cells using cytokeratin. Scattered macrophages (CD68, red), T cells (CD3, cyan) and activated T cells (CD44, yellow) are also present. In contrast, the explant liver (patient CVR35) in **b** shows prominent proliferation of epithelial cells throughout the liver tissue (green), with increased macrophages (red), T cells (cyan) and activated T cells (yellow). In panel **c**, the control liver shows scattered cytotoxic T (CD8, red), CD107a positive (brown) and CD4 positive (yellow) cells and low expression of the interferon-induced GTP-binding protein Mx-1(green), compared to high numbers of all cell types and high Mx-1 expression in the explant patient **d**. Bars (**a-d**), 50 micrometres. One section of liver was stained per subject, and the entire area was outlined manually. Cells were segmented to identify the nuclei and cytoplasm, and the algorithm was tuned to detect the colour signal in the cells. All samples were analysed with the same algorithm for each stain.

Extended data legends

Extended Data Figure 1 | AAV2, HAdV and human herpesvirus detection by target enrichment sequencing in cases and controls. Read counts per million are plotted for a) HAdV; b) AAV2; c) HHV6B; d) HSV1; e) HSV2; f) VZV; g) HHV6A; h) HHV7; i) HHV8; and j) CMV in cases, Group 1 healthy controls and Group 2 controls (HAdV positive children with normal liver function). Statistical significance was estimated using a Mann-Whitney test (two-sided).

Extended Data Figure 2 | Phylogenetic and sequence analysis of AAV2 genomes. a) Maximum likelihood phylogeny of AAV2 from hepatitis cases CVR1-9. The nine AAV2 genome sequences generated from the plasma samples via target enrichment (highlighted in green) were aligned with a range of the closest AAV GenBank sequences[33]**.** AAV2 reference

sequences are denoted by accession number, country and year of sampling b,) Phylogeny of HAdV41 genome from case 5. The HAdV41 genome sequence from the faecal sample of patient 5 (red) was combined with complete genomes of HAdV41 from GenBank. Bootstrap values >70 are indicated. HAdV41 reference sequences are denoted by accession number, country and year of sampling; c,) Key mutations and hierarchical clustering of AAV2 genomes. Mutations in published AAV2 sequences are highlighted in (blue) and case sequences (green); d) Mutations over-represented in hepatitis cases versus controls. Mutations in VP1-3, Rep78 and 52 and AAP are highlighted by % representation in case sequences (green) and published sequences (blue).

Extended Data Figure 3 | AAV2 viraemia and liver function over time. Panel a) shows bilirubin and AAV2 viraemia while panel b) shows alanine transaminase (ALT) plotted over time (days post-date of first reported symptom(s)).

Extended Data Figure 4 | Reactivity of sera from paediatric hepatitis cases against human seasonal coronaviruses and SARS-CoV-2. Sera from the paediatric hepatitis cases were screened for reactivity against spike proteins from **a)** seasonal coronaviruses 229E, OC43, NL63 and HKU1, and **b**) SARS-CoV-2 nucleocapsid (N), spike (S), and N-terminal domain (NTD) and receptor binding domain (RBD) of S by electrochemiluminescence (MSD-ECL). Reactivity of the 23 samples (Hepatitis) was compared with 16 sera from contemporaneous control samples from children (Group 4 Controls), and three groups of sera from adults of known SARS-CoV-2 status; Negatives (never tested positive for SARS-CoV-2; n=30), Vaccinated two doses (n=28) and Infected (n=39).

Extended Data Figure 5 | Principal component analysis (PCA) plots showing the first four genome-wide principal components to confirm genetic ancestry matching. **a)** Genomic PCA using full UK Biobank cohort as background population (grey), showing the subgroup of unrelated UK Biobank participants who were born in Scotland and of Caucasian ancestry (blue) and the hepatitis cases reported here (red). **b)** plots showing only the subgroup born in Scotland and of Caucasian ancestry.

Extended Data Figure 6 | Quantification of immune cells in liver cases and adult controls. The percentage of positively immuno-stained cells were quantified in whole scanned slides of liver tissue. a) B cells (CD20), **b)** CD8 T cells, and **c)** CD3 T cells were analysed, respectively. The red data point represents data from the explant liver (CVR35). The bar shows the median.

Methods

ISARIC CCP-UK recruitment, Biorepository & DIAMONDS studies

Ethical approval for the ISARIC CCP-UK study was given by the South Central–Oxford C Research Ethics Committee in England (13/SC/0149), the Scotland A Research Ethics Committee (20/SS/0028), and the WHO Ethics Review Committee (RPC571 and RPC572). Thirty-two children aged <16 years were recruited prospectively by written informed consent (parent or guardian) from the ISARIC WHO CCP-UK cohort admitted to hospital with elevated transaminases (defined as ALT >400 IU/L and/or AST >400 IU/L) that was not due to viral hepatitis A-E, autoimmune hepatitis or poisoning. Nine cases had available clinical samples for further investigation. Three further cases had HLA typing performed but samples were not available for further analysis. Control samples were obtained from children (aged

<16 years) recruited to the Diagnosis and Management of Febrile Illness using RNA Personalised Molecular Signature Diagnosis (DIAMONDS), an ongoing multi-country study that aims to develop a molecular diagnostic test for the rapid diagnosis of severe infection and inflammatory diseases using personalised gene signatures (ISRCTN12394803). Ethical approval was given by London-Dulwich Research Ethics Committee (20/HRA/1714). Controls included healthy controls (n=13; Group 1), children with PCR-confirmed adenoviral infection with normal transaminases (n=12; Group 2), and children with raised transaminases without adenoviral infection (n=33; Group 3), recruited between 19 May 2020 to 8 January 2022. Scottish surplus plasma (aged <10 years; March to April 2022; Group 4) and liver biopsy control samples (aged <18 years; January 2021-July 2022) from the Diagnostic Pathology/Blood Sciences archive were obtained with NHS GG&C Biorepository approval (application #717; REC 22/WS/0020). Negative control adult samples that had tested negative by PCR for SARS-CoV-2 were used as an additional group for serological analysis of coronaviruses, also with NHS GG&C Biorepository approval. These samples were used without consent following HTA legislation on consent exemption.

Viral PCR

RNA extraction was carried out using the Biomerieux Easymag generic protocol. 300ul of plasma or sera was extracted and eluted into 80 ul of water.

AAV2 qRT-PCR was performed to detect a 62bp amplicon of the AAV2 inverted terminal repeat region (ITR) as previously described[32] using the forward ITR primer 5'-GGAACCCCTAGTGATGGAGTT-3') and the reverse ITR primer 5'-CGGCCTCAGTGAGCGA-3'). The AAV2 ITR hydrolysis probe was labelled with

618 fluorescein (6FAM) and quenched with Black Hole quencher (BHQ) 5'-[6FAM]-
619 CACTCCCTCTCTGCGCGCTCG-[BHQ1]3'). AAV2 primers and probe were synthesised
620 by Merck Life Sciences UK Limited, United Kingdom. qRT-PCR analysis was performed
621 using the ABI7500 Fast Real-Time PCR system (Applied Biosystems). LUNA Universal
622 One-Step RT PCR kit (New England Biolabs) was used for the amplification and detection of
623 the AAV2 ITR target. qRT-PCR reactions were performed in a 20µl volume reaction (Luna
624 Universal One-Step reaction mix, Luna WarmStart RT enzyme mix, 400nM forward and
625 reverse primers, 200nM AAV2 ITR probe and 1-2.5µl of template DNA) as per
626 manufacturer's instructions. To quantify the number of copies, serial dilutions of plasmid
627 containing the 62bp ITR product were used to generate a standard curve which was then used
628 to interpolate the copy number of AAV2 copies in the samples. Wells with no template were
629 used as negative controls. qRT-PCR reactions were performed in triplicate. The qRT-PCR
630 program consisted of an initial reverse transcription step at 55 C for 10 minutes, an initial
631 denaturation at 95 C for 1 minute followed by 45 cycles 95 C denaturation for 10 seconds and
632 extension at 58 C for 1 minute. A qPCR detection limit between 31 and 32 cycles was
633 calculated as the threshold Ct value at the last dilution of DNA standards that were within the
634 linear range. A PCR result was considered positive if all three reactions tested positive at
635 ≤31 cycles.
636
637 Digital droplet PCR (ddPCR) was performed according to the manufacturer's instructions
638 using the ddPCR Supermix for Probes (No dUTP) (Bio-Rad, UK cat no. 1863023) and
639 analysed using an QX200 Droplet Digital PCR system (Bio-Rad, UK cat no. 1864001)

640 The West of Scotland Specialist Virology Centre, NHS Greater Glasgow and Clyde
641 conducted diagnostic real-time PCR with reverse transcription to detect HAdV, SARS-CoV-
642 2-positive samples and other viral pathogens associated with hepatitis (e.g. Hepatitis A-E),

following nucleic acid extraction utilizing the NucliSENS easyMAG and Roche MG96 platforms. HHV6[2] and HAdV41[33] were tested by qPCR as previously described using Invitrogen platinum qPCR mix (Cat no 11730-025) and Quanta Biosciences qPCR mix Mastermix (Cat.No. 733-1273) respectively on an ABI7500 and amplified for 40 cycles. A 6ul extract was amplified in a total reaction volume of 15ul.

Measurement of antibody response to coronaviruses by electrochemiluminescence

IgG antibody titres were measured quantitatively against SARS-CoV-2 spike (S) protein, N-terminal domain (NTD), receptor binding domain (RBD) or nucleocapsid (N), and the spike glycoproteins of human seasonal coronaviruses (HCoVs) 229E, OC43, NL63 and HKU1 using MSD V-PLEX COVID-19 Coronavirus Panel 2 (K15369) and Respiratory Panel 1 (K15365) kits. Multiplex Meso Scale Discovery electrochemiluminescence (MSD-ECL) assays were performed according to manufacturer instructions. Samples were diluted 1:5000 in diluent and added to the plates along with serially diluted reference standard (calibrator) and serology controls 1.1, 1.2 and 1.3. Plates were read using a MESO Sector S 600 plate reader. Data were generated by Methodological Mind software and analysed using MSD Discovery Workbench (v4.0). Results are expressed as MSD arbitrary units per ml (AU/ml). Adult negative and positive pools gave the following values: Negative pool - spike 56.6 AU/ml, NTD 119.4 AU/ml, RBD 110.5 AU/ml and nucleocapsid 20.7 AU/ml; SARS-CoV-2 Positive pool – spike 1331.1 AU/ml, NTD 1545.2 AU/ml, RBD 1156.4 AU/ml and nucleocapsid 1549.0 AU/ml. In the same assay, NIBSC 20/130 reference serum – spike 547.7 AU/ml, NTD 538.8 AU/ml, RBD 536.9 AU/ml and nucleocapsid 1840.2 AU/ml.

Metagenomic sequencing

Full protocols on the discovery of RNA and DNA viruses using metagenomic next-generation sequencing and target enrichment sequencing methods can be found at the following sites:

dx.doi.org/10.17504/protocols.io.261ge34zol47/v1

dx.doi.org/10.17504/protocols.io.36wgqj3q3vk5/v1

In summary, residual nucleic acid from 27 samples (9 patients with a combination of plasma, liver, faeces, rectal and throat/nose samples), 12 HAdV-positive and 13 healthy controls (control samples were either plasma or sera) underwent metagenomic next-generation sequencing at the CVR. Briefly, each nucleic acid sample was split in two library preparations, to improve the chances of detecting RNA and DNA viruses. The protocol applied for improved detection of RNA viruses included treatment with DNaseI (Ambion DNase I, ThermoFisher), ribosomal depletion (Ribo-Zero Plus rRNA Depletion Kit, Illumina), except for plasma samples, reverse transcription (SuperScript III, Invitrogen) and double-strand DNA synthesis (NEBNext® Ultra™ II Non-Directional RNA Second Strand Synthesis Module, NEB). The protocol applied to detect DNA viruses included partial removal of host DNA (NEBNext® Microbiome DNA Enrichment Kit, NEB). Following this, both sets of samples were used to prepare libraries using the KAPA LTP kit (Roche) with unique dual indices (NEBNext® Multiplex oligos for Illumina, NEB). The resulting libraries were pooled in equimolar amounts and sequenced using a NextSeq500 (Illumina) to obtain paired end reads using 150X150 cycles.

Target enrichment sequencing

Following on the library preparation step described above, DNA and RNA derived libraries were pooled separately and were incubated with the VirCapSeq-VERT Capture Panel probes (Roche) following the manufacturer's guidelines. The Roche VirCapSeq-VERT Capture

Panel covers the genomes of 207 viral taxa known to infect vertebrates (including humans). Enriched DNA and RNA- derived libraries were further amplified using 14 PCR cycles, pooled and sequenced using a NextSeq500 (Illumina) to obtain paired end reads using 150X150 cycles.

Bioinformatics analysis

Reads for each sample were first quality checked, Illumina adapters were trimmed using Trim Galore (https://github.com/FelixKrueger/TrimGalore) and then mapped to the human genome using BWA-MEM (https://github.com/lh3/bwa). Only reads that did not map to the human genome were used for metagenomic analyses. Reads per million were calculated as the number of viral reads per million reads sequenced, to normalise for variation in sample sequencing depth. Non-human reads were then *de novo* assembled using MetaSPAdes (https://github.com/ablab/spades) to generate contigs for each sample. Contigs were compared against a protein database of all NCBI RefSeq organisms (including virus, bacteria, eukaryotes) with BLASTX using DIAMOND (https://github.com/bbuchfink/diamond). In addition, non-human reads for each sample were aligned to a small panel of HAdV NCBI RefSeq genomes (HAdV-A, B1, B2, C, D, E, F, 1, 2, 5, 7, 35, 54 as well as HAdV-F41).

The nine AAV2 near-complete genome contigs from the plasma samples were assembled and compared with sequences in GenBank using BLASTN (nucleotide database). Each of these AAV2 genomes had numerous close hits (exhibiting >95% similarity across 95% of the genome) with various existing AAV2 sequences; those most closely related were reported in a recent publication[31] All linear complete AAV2 genomes returned via BLAST against the GenBank nt database with a query coverage >75%, were selected and combined with the AAV sequences *de novo* assembled here and aligned with MAFFT. The terminal ends of this

alignment were trimmed off and IQ-TREE 2 was used (TIM+F+R3 model) to infer a phylogenetic tree. For the single HAdV41 genome *de novo* assembled, all available HAdV41 complete genomes were downloaded from GenBank, aligned with MAFFT and IQ-TREE2 was used (K2P+R2 model) to infer a phylogenetic tree.

Anti-AAV2 ELISA Assay

AAV2 pAAV-CAG-tdTomato viral preparation (codon diversified) was a gift from Edward Boyden (Addgene viral prep #59462-AAV2; http://n2t.net/addgene:59462; RRID:Addgene_59462).

AAV2 particles, obtained from Addgene (cat. No. 59462-AAV2, Addgene, UK), were diluted in PBS and used to coat a Immulon 2HB 96-well flat bottom plate (ImmunoChemistry Technologies, LLC, CA, USA) at a concentration of $1x10^8$ particles per well. The plates were incubated on an orbital shaker overnight at 4^0C. Plates were then blocked with PBS-T (PBS, 0.1% Tween20) containing 5% BSA for 1 hour prior to the addition on samples. The plates were washed five times in PBS-T before serum samples, diluted 1:50 in PBS, were added in triplicate. A mouse anti-AAV2 (A20, Progen, Germany) was used as a positive control at a concentration of 1:50. Samples were incubated at room temperature on an orbital shaker for 1:30 hrs before washing five times in PBS-T and adding either Anti-Human IgM or Anti-Human IgG (Merck, UK cat no. A9794 and A1543, respectively) diluted 1:10000, Goat Anti-Mouse IgG (Merck, UK cat no. A2429) was used as the secondary for the anti AAV2 A20 positive control. The plates were incubated for 1hr before washing five times with PBS-T then 100ul of Alkaline Phosphatase yellow (Merck, UK cat no. P7998) was added an incubated for 15 minutes before stopping the reaction with 3M NaOH and measuring absorbance at 405nm.

Immunohistochemistry, in situ-hybridization, and special staining

Formalin-fixed and paraffin-wax embedded liver samples were cut at ~3 micrometre thickness and mounted on glass slides. A reticulin (1936) and Masson trichrome (1929) special staining (Gordon and Sweets method (1936)) was performed. Antibodies used for immunohistochemistry are listed in Supplementary Table 6.

Detection of viral nucleic acids as well as ubiquitin and DapB-specific RNA (Advanced Cell Diagnostics, AAV2 (1195791), HHV6 (144565), Adenovirus 41 (1192351, Ubiquitin (310041) and DapB (310043)) was performed following the manufacturer's protocol with pretreatment with simmering in target solution (30 min) and additional proteinase K (30 min.) treatment. A haematoxylin counterstain was performed, and slides were mounted with Vectamount mounting media (# H-500, Vector Laboratories) and scanned with a bright field slide scanner (Leica, Aperio Versa 8).

Liver histopathology grading

Liver scoring was performed as previously described[8,9].

Quantification of immune cells

After scanning of the whole slides, liver tissue was outlined and the number of positively stained cells (DAB signal for immunohistochemistry or Fast Red signal for *in situ*-hybridization) was assessed using software assisted image analysis (QuPath version 0.3.2)[34]. For each marker, the cell detection algorithm was tuned, and data plotted in Graph Pad Prism (version 9.4.1).

Spatial analysis (Codex Phenocycler)

Formalin fixed, paraffin-wax embedded liver samples (patient 228742A and 145808) were sectioned at 2 to 4 micrometre thickness on 22 mm x 22 mm glass coverslips (Akoya Biosciences, #7000005) coated in 0.1% poly-L-lysine (Sigma-Aldrich, Cat. P8920). Antigen retrieval was performed by pressure cooking with citrate buffer at pH 6. Carrier-free, pre-conjugated antibodies were purchased directly from Akoya Biosciences or purchased from other suppliers in preparation for custom-conjugation**.** If carrier-free antibodies were not available, alternatives were purchased and purified using a Pierce™ antibody cleanup kit (Ref #44600, Thermofisher). Antibodies were custom conjugated to a unique oligonucleotide barcode according to manufacturer's instructions using an antibody conjugation kit (Ref #7000009, Akoya Biosciences) and stored at 4°C for at least 48 hours before use. Conjugated antibodies were stored at 4°C.

Coverslips with tissue were rehydrated in an alcohol series and washed in distilled water, before performing heat-induced antigen retrieval in a pressure cooker with citrate buffer (pH 6). Glass coverslips were then moved progressively between wells of a 6-well plate containing components of the CODEX staining kit (Akoya Biosciences, #7000008). This included 2 wells of hydration buffer (2 mins each), 1 well of staining buffer (20 mins), and then staining with 190ul of an 11-marker antibody panel **(**Supplementary Table 7**)**. Tissue sections of both samples were treated in the same way on the same day and were incubated with antibodies for 3 hours at room temperature (RT) simultaneously. Following staining, tissue was incubated twice in staining buffer (2 min each) and transferred to a post-staining fixation solution made from a 1:10 ratio of PFA:storage buffer fo r 10 mins. Tissues were then washed 3 times in 1X phosphate buffered saline (PBS; #14190-094, Gibco), incubated in ice-cold methanol (# M/4000/PC17, Fisher scientific) for 5 mins on ice, and again washed 3

785 times in PBS. Tissue sections were fixed in a fixative solution for 20 mins, washed 3x in PBS
786 and stored in storage buffer until image acquisition

787 Image acquisition was achieved using a Keyence BZ-X710 microscope equipped with 4
788 fluorescent channels (one nuclear stain, 3 for antibody visualization). In a 96-well plate
789 (Akoya Biosciences, #7000006), a maximum of three oligonucleotide reporters are used per
790 well (cycle) (5 microlitre each) and added to between 235 microlitre -245microlitre reporter
791 stock solution created according to manufacturer's instructions. Plates were sealed with
792 aluminum film (Akoya Biosciences, #7000007) and stored at 4°C until use. Pictures were
793 captured with QuPath version 0.3.2 https://www.nature.com/articles/s41598-017-17204-5.

794

795 ***Host genetics and HLA typing***

796 High resolution typing for all HLA loci (HLA-A, B, C, DRB1, DRB3/4/5, DQA1, DQB1,
797 DPA1 and DPB1) was performed using AllType™ FASTplex™ NGS Assay (One Lambda)
798 run on an Illumina Mi-Seq platform. HLA typing was undertaken on 27 ISARIC consented
799 patients. One patient was omitted from analysis as they were a sibling of another case. HLA
800 types from 64 Scottish National Blood Transfusion Service apheresis platelet donors, self-
801 identified as White British (n=15) or White Scottish (n=49) were used as control samples for
802 comparison with patient HLA allele frequencies. Genotyping was performed using the
803 Illumina Global Screening Array v3.0 + multi-disease beadchips (GSAMD-24v3-0-EA) and
804 Infinium chemistry. This consists of three steps: (1) whole genome amplification, (2)
805 fragmentation followed by hybridisation, and (3) single-base extension and staining. Arrays
806 were imaged on an Illumina iScan platform and genotypes were called automatically using

GenomeStudio Analysis software v2.0.3, GSAMD-24v3-0-EA_20034606_A1.bpm manifest and cluster file provided by manufacturer.

Given the small sample size, it was not possible to implement quality control processes using GenomeStudio and manufacturer's published recommendations. As genotyping was conducted using the same genotyping array used for the genOMICC study, variants that passed quality control for the genOMICC study were retained, as described previously[35]. After further excluding variants with call rates <95%, a total of 478,692 variants was used for downstream analysis.

Kinship and population structure

To identify close relatives up to 3rd degree King 2.1 was used, confirming the presence of a pair of siblings with no further close relatives identified. Genotypes of 19 patients were combined with imputed genotypes of a subset of unrelated UK Biobank participants obtained by removing one individual in each pair with estimated kinship larger than 0.0442. The resulting genotypes were filtered to exclude variants with MAF < 5%, genotype missingness rate < 1.5%, and Hardy–Weinberg equilibrium (HWE) $P < 10^{-50}$. Principal component analysis (PCA) was conducted with gcta 1.955 in the set of unrelated individuals with pruned SNPs using a window of 1,000 markers, a step size of 50 markers and an r2 threshold of 0.01. Analyses were performed once including all UK Biobank participants and once including only UK Biobank participants who were born in Scotland (UKB Field 1647) and of Caucasian genetic ancestry (UKB Field 22006).

Statistics

Differences between cases and control groups were tested using Fisher's Exact Test for categorical variables and Mann-Whitney (two tailed) for continuous variables respectively using R studio version 1.2.5033, R version 4.1.2 and GraphPad version 9.0.0.

For coronavirus serology experiments, comparisons were carried out with one way ANOVA and Tukey's Multiple Comparison test, carried out in GraphPad version 8.4.3.

HLA analysis used the Bridging ImmunoGenomic Data-Analysis Workflow Gaps (BIGDAWG) R package to derive OR and corrected p values for individual HLA alleles[36]. Bonferroni corrected p value significance threshold, adjusted for multiple comparisons (168 HLA alleles), was $p<3.0\times10^{-4}$.

Figures

Figures were prepared using Microsoft Office Excel 2010, Microsoft Office Powerpoint 2010 and Adobe Illustrator 2022.

Data availability

Datasets generated in the current study are appended as Extended Datasets, Source Data and Supplementary Tables. Data, protocols, and all documentation around this analysis may be made available to academic researchers after authorisation from the independent data access and sharing committee. Clinical data and analysis scripts are available on request to the Independent Data Management and Access Committee at https://isaric4c.net/ sample_access. Restrictions apply to the availability of identifiable clinical data. Due to the relatively small number of cases, de-aggregation of data is potentially disclosive, as is the patient-level line list data. Therefore, a formal data sharing agreement is required for data access. The

Independent Data and Material Access Committee considers requests as they arrive; most responses are made within 28 days. Use of clinical samples are also restricted under ethical approvals obtained for their use. Genome sequences are available in GenBank with accession numbers for AAV2: OP019741-OP019749 and for HAdV-F41: OP019750.

Code availability

Freely available bioinformatics and statistical software were used, see links in the Methods section.

References

1 Marsh, K. *et al.* Investigation into cases of hepatitis of unknown aetiology among young children, Scotland, 1 January 2022 to 12 April 2022. *Euro Surveill* **27**, doi:10.2807/1560-7917.ES.2022.27.15.2200318 (2022).

2 World Health Organization. *Severe acute hepatitis of unknown aetiology in children - Multi-country*, <https://www.who.int/emergencies/disease-outbreak-news/item/2022-DON400> (2022).

3 UK Health Security Agency. Investigation into acute hepatitis of unknown aetiology in children in England - Technical Briefing 4. (UKHSA, 2022).

4 Gutierrez Sanchez, L. H. *et al.* A Case Series of Children with Acute Hepatitis and Human Adenovirus Infection. *N Engl J Med*, doi:10.1056/NEJMoa2206294 (2022).

5 Karpen, S. J. Acute Hepatitis in Children in 2022 - Human Adenovirus 41? *N Engl J Med*, doi:10.1056/NEJMe2208409 (2022).

6 Kelgeri, C. *et al.* Clinical Spectrum of Children with Acute Hepatitis of Unknown Cause. *N Engl J Med*, doi:10.1056/NEJMoa2206704 (2022).

7 Dunning, J. W. *et al.* Open source clinical science for emerging infections. *Lancet Infect Dis* **14**, 8-9, doi:10.1016/S1473-3099(13)70327-X (2014).

8 Knodell, R. G. *et al.* Formulation and application of a numerical scoring system for assessing histological activity in asymptomatic chronic active hepatitis. *Hepatology* **1**, 431-435, doi:10.1002/hep.1840010511 (1981).

9 Krishna, M. Histological Grading and Staging of Chronic Hepatitis. *Clin Liver Dis (Hoboken)* **17**, 222-226, doi:10.1002/cld.1014 (2021).

10 Public Health Scotland. *Enhanced Surveillance of Covid-19 in Scotland (Population-based seroprevalence) - 5 week rolling estimate.*, <https://publichealthscotland.scot/publications/enhanced-surveillance-of-covid-19-in-scotland/enhanced-surveillance-of-covid-19-in-scotland-population-based-seroprevalence-surveillance-1-june-2022/dashboard/> (2022).

11 Rodriguez-Inigo, E. *et al.* Percentage of hepatitis C virus-infected hepatocytes is a better predictor of response than serum viremia levels. *J Mol Diagn* **7**, 535-543, doi:10.1016/S1525-1578(10)60585-5 (2005).

12 Tomlinson, J. E. *et al.* Tropism, pathology, and transmission of equine parvovirus-hepatitis. *Emerg Microbes Infect* **9**, 651-663, doi:10.1080/22221751.2020.1741326 (2020).

13 Leen, G., Stein, J. E., Robinson, J., Maldonado Torres, H. & Marsh, S. G. E. The HLA diversity of the Anthony Nolan register. *HLA* **97**, 15-29, doi:10.1111/tan.14127 (2021).

14 Srivastava, A., Lusby, E. W. & Berns, K. I. Nucleotide sequence and organization of the adeno-associated virus 2 genome. *J Virol* **45**, 555-564, doi:10.1128/JVI.45.2.555-564.1983 (1983).

15 Atchison, R. W., Casto, B. C. & Hammon, W. M. Adenovirus-Associated Defective Virus Particles. *Science* **149**, 754-756, doi:10.1126/science.149.3685.754 (1965).

16 Li, C. *et al.* Neutralizing antibodies against adeno-associated virus examined prospectively in pediatric patients with hemophilia. *Gene Ther* **19**, 288-294, doi:10.1038/gt.2011.90 (2012).

17 Martino, A. T. *et al.* Engineered AAV vector minimizes in vivo targeting of transduced hepatocytes by capsid-specific CD8+ T cells. *Blood* **121**, 2224-2233, doi:10.1182/blood-2012-10-460733 (2013).

18 Manno, C. S. *et al.* Successful transduction of liver in hemophilia by AAV-Factor IX and limitations imposed by the host immune response. *Nat Med* **12**, 342-347, doi:10.1038/nm1358 (2006).

19 Mingozzi, F. *et al.* CD8(+) T-cell responses to adeno-associated virus capsid in humans. *Nat Med* **13**, 419-422, doi:10.1038/nm1549 (2007).

20 Ertl, H. C. J. Immunogenicity and toxicity of AAV gene therapy. *Front Immunol* **13**, 975803, doi:10.3389/fimmu.2022.975803 (2022).

21 Chowdary, P. *et al.* Phase 1-2 Trial of AAVS3 Gene Therapy in Patients with Hemophilia B. *N Engl J Med* **387**, 237-247, doi:10.1056/NEJMoa2119913 (2022).

22 Sebode, M., Weiler-Normann, C., Liwinski, T. & Schramm, C. Autoantibodies in Autoimmune Liver Disease-Clinical and Diagnostic Relevance. *Front Immunol* **9**, 609, doi:10.3389/fimmu.2018.00609 (2018).

23 Rafie, K. *et al.* The structure of enteric human adenovirus 41-A leading cause of diarrhea in children. *Sci Adv* **7**, doi:10.1126/sciadv.abe0974 (2021).

24 Echavarria, M. Adenoviruses in immunocompromised hosts. *Clin Microbiol Rev* **21**, 704-715, doi:10.1128/CMR.00052-07 (2008).

25 Baker, J. M. *et al.* Acute Hepatitis and Adenovirus Infection Among Children - Alabama, October 2021-February 2022. *MMWR Morb Mortal Wkly Rep* **71**, 638-640, doi:10.15585/mmwr.mm7118e1 (2022).

26 Cooper, S. *et al.* Long COVID-19 Liver Manifestation in Children. *J Pediatr Gastroenterol Nutr*, doi:10.1097/MPG.0000000000003521 (2022).

27 Deep, A., Grammatikopoulos, T., Heaton, N., Verma, A. & Dhawan, A. Outbreak of hepatitis in children: clinical course of children with acute liver failure admitted to the intensive care unit. *Intensive Care Med*, doi:10.1007/s00134-022-06765-3 (2022).

28 van Gerven, N. M. *et al.* HLA-DRB1*03:01 and HLA-DRB1*04:01 modify the presentation and outcome in autoimmune hepatitis type-1. *Genes Immun* **16**, 247-252, doi:10.1038/gene.2014.82 (2015).

29 Lanchbury, J. S. *et al.* Strong primary selection for the Dw4 subtype of DR4 accounts for the HLA-DQw7 association with Felty's syndrome. *Hum Immunol* **32**, 56-64, doi:10.1016/0198-8859(91)90117-r (1991).

30 Gay, D. *et al.* Functional interaction between human T-cell protein CD4 and the major histocompatibility complex HLA-DR antigen. *Nature* **328**, 626-629, doi:10.1038/328626a0 (1987).

31 La Bella, T. *et al.* Adeno-associated virus in the liver: natural history and consequences in tumour development. *Gut* **69**, 737-747, doi:10.1136/gutjnl-2019-318281 (2020).

Methods References

32 Aurnhammer, C. *et al.* Universal real-time PCR for the detection and quantification of adeno-associated virus serotype 2-derived inverted terminal repeat sequences. *Hum Gene Ther Methods* **23**, 18-28, doi:10.1089/hgtb.2011.034 (2012).

33 Gautheret-Dejean, A. *et al.* Development of a real-time polymerase chain reaction assay for the diagnosis of human herpesvirus-6 infection and application to bone marrow transplant patients. *J Virol Methods* **100**, 27-35, doi:10.1016/s0166-0934(01)00390-1 (2002).

34 Bankhead, P. *et al.* QuPath: Open source software for digital pathology image analysis. *Sci Rep* **7**, 16878, doi:10.1038/s41598-017-17204-5 (2017).

35 Pairo-Castineira, E. *et al.* Genetic mechanisms of critical illness in COVID-19. *Nature* **591**, 92-98, doi:10.1038/s41586-020-03065-y (2021).

36 Pappas, D. J., Marin, W., Hollenbach, J. A. & Mack, S. J. Bridging ImmunoGenomic Data Analysis Workflow Gaps (BIGDAWG): An integrated case-control analysis pipeline. *Hum Immunol* **77**, 283-287, doi:10.1016/j.humimm.2015.12.006 (2016).

968

969 **Acknowledgements**

970 We wish to acknowledge the contribution of the participating children and their parents who
971 agreed to participate in the ISARIC CCP-UK and DIAMONDS studies, and the research
972 teams who recruited the patients.

973

974 The work was funded by Public Health Scotland, the National Institute for Health Research
975 (NIHR; award CO-CIN-01) and the Medical Research Council (MRC; grants
976 MR/X010252/1, MC_UU_1201412, MC_UU_12018/12, MC_PC_19059, MC_PC_19025 &
977 MC_PC_22004). DIAMONDS is funded by the European Union Horizon 2020 programme;
978 grant 848196). MP acknowledges funding support from the Wellcome Trust
979 (206369/Z/17/Z). MGS gratefully acknowledges funding support from The
980 Pandemic Institute, Liverpool and the NIHR Health Protection Research Unit (HPRU) in
981 Emerging and Zoonotic Infections at University of Liverpool, and UK Health Security
982 Agency (UKHSA). JKB gratefully acknowledges funding support from a Wellcome Trust
983 Senior Research Fellowship (223164/Z/21/Z), and MC_PC_20029, Sepsis Research (Fiona
984 Elizabeth Agnew Trust), a BBSRC Institute Strategic Programme Grant to the Roslin
985 Institute (BB/P013732/1, BB/P013759/1), and the UK Intensive Care Society. We gratefully
986 acknowledge the support of Baillie Gifford and the Baillie Gifford Science Pandemic Hub at
987 the University of Edinburgh. Parts of this research has been conducted using the UK Biobank
988 Resource under project 788 and we would like to acknowledge the assistance of Prof. Albert
989 Tenesa in making this possible. Additional replication was also conducted using the UK
990 Biobank Resource (Project 26041).We also acknowledge the support of NHS Research
991 Scotland (NRS) Greater Glasgow and Clyde Biorepository team. The authors would like to
992 thank the histopathology team, Veterinary Diagnostic, University of Glasgow, for excellent

technical assistance. We acknowledge Pablo Murcia for providing resources and advice and Paula Olmo for administrative assistance. Lastly, we acknowledge the invaluable advice of Eric J. Kremer from the Institut de Génétique Moléculaire de Montpellier, Université de Montpellier and Andrew Baker, University of Edinburgh.

Author contributions

AH, AdSF, JKB, ECT conceived the study. AH, RO, PA, VH, CD, BW, DT, RB, JH, PH, SR, CW and ECT did the formal analysis. AH, RT, PA, VH, CD, LT, KS, MM, JA, BW, KR, LP, LG, CE, JM, KR, KM, TD, MH, ML, DY, SC, MO'L, DH, AM, NM, AdSF, JB, DT, RB, PH, MO, PC, WO, MC and ECT did the investigation. SEM, EV, TD, SS, CJ, RG, AM, NM, AB-S, MSH, DE-R, ML provided resources. NA, EP-C and VV performed validation. AH and ECT wrote the original draft of the manuscript. AH, RO, RT, PA, LP, JM, KR, KM, TD, MH, ML, PH, MC, ML, MP, DLR, AdSF, BW, JB, MGS, DT, JKB and ECT reviewed and edited the manuscript. RO, PA, VH, CD, KR, BW and ECT visualised the data.

Competing interest declaration

The authors have no competing interests

Additional Information

Supplementary Information is available for this paper.

Correspondence and requests for materials should be addressed to Professor Emma C Thomson.

.

Reprints and permissions information is available at www.nature.com/reprints.

CONSORTIA

ISARIC Comprehensive Clinical Characterisation Collaboration (ISARIC4C)

J Kenneth Baillie[1,2,3], Malcolm G Semple[4,5], Gail Carson[6], Peter JM Openshaw[7,8], Jake Dunning[9,7], Laura Merson[6], Clark D Russell[10], David Dorward[11], Maria Zambon[9], Meera Chand[12], Richard S Tedder[13,14,15], Saye Khoo[16], Lance CW Turtle[4,17], Tom Solomon[4,18], Samreen Ijaz[9], Tom Fletcher[19], Massimo Palmarini[20], Antonia Ho[20,21], Emma C Thomson[20], Nicholas Price[22,23], Judith Breuer[24], Thushan de Silva[25], Chloe Donohue[26], Hayley Hardwick[4], Wilna Oosthuyzen[27], Miranda Odam[27], Primrose Chikowore[27], Lauren Obosi[27], Sara Clohisey[27], Andrew Law[27], Lucy Norris[28], Sarah Tait[29], Murray Wham[3], Richard Clark[30], Audrey Coutts[30], Lorna Donnelly[30], Angie Fawkes[30], Tammy Gilchrist[30], Katarzyna Hafezi[30], Louise MacGillivray[30], Alan Maclean[30], Sarah McCafferty[30], Kirstie Morrice[30], Lee Murphy[30], Nicola Wrobel[30], Sarah E McDonald[20], Victoria Shaw[31], Katie A. Ahmed, Jane A Armstrong[32], Lauren Lett[33], Paul Henderson[34], Louisa Pollock[35], Shyla Kishore[36], Helen Brotherton[37], Lawrence Armstrong[38], Andrew Mitra[39], Anna Dall[40], Kristyna Bohmova[41], Sheena Logan[41], Louise Gannon[42], Ken Agwuh[43], Srikanth Chukkambotla[44], Ingrid

DuRand[45], Duncan Fullerton[46], Sanjeev Gar[47], Clive Graham[48], Tassos Grammatikopoulos[49,50], Stuart Hartshorn[51], Luke Hodgson[52], Paul Jennings[53], George Koshy[54], Tamas Leiner[54], James Limb[55], Jeff Little[56], Sheena Logan, Elijah Matovu[46], Fiona McGill[57], Craig Morris[58], John Morrice[59], David Price[60], Henrik Reschreiter[61], Tim Reynolds[58], Paul Whittaker[62], Thomas Jordan[37], Rachel Tayler[63], Clare Irving[64], Katherine Jack, Maxine Ramsay[65], Margaret Millar[65], Barry Milligan[66], Naomi Hickey[66], Maggie Connon[36], Catriona Ward[36], Laura Beveridge[59], Susan MacFarlane[42], Karen Leitch[37], Claire Bell[67], Lauren Finlayson[40], Joy Dawson[40], Janie Candlish[39], Laura McGenily[41], Tara Roome[51], Cynthia Diaba[68], Jasmine Player[69], Natassia Powell[70], Ruth Howman[51], Sara Burling[51], Sharon Floyd[52], Sarah Farmer[43], Susie Ferguson[71], Susan Hope[72], Lucy Rubick[61], Rachel Swingler[73], Emma Collins[74], Collette Spencer[57], Amaryl Jones[46], Barbara Wilson[75], Diane Armstrong[76], Mark Birt[77], Holly Dickinson[58], Rosemary Harper[76], Darran Martin[78], Amy Roff[61], Sarah Mills[61]

1. Roslin Institute, University of Edinburgh, Easter Bush, Edinburgh, EH25 9RG, UK
2. Intensive Care Unit, Royal Infirmary Edinburgh, Edinburgh, UK
3. MRC Human Genetics Unit, MRC Institute of Genetics and Molecular Medicine, University of Edinburgh, Edinburgh, UK
4. NIHR Health Protection Research Unit, Institute of Infection, Veterinary and Ecological Sciences, Faculty of Health and Life Sciences, University of Liverpool, Liverpool, UK
5. Respiratory Medicine, Alder Hey Children's Hospital, Institute in The Park, University of Liverpool, Alder Hey Children's Hospital, Liverpool, UK

6. ISARIC Global Support Centre, Centre for Tropical Medicine and Global Health, Nuffield Department of Medicine, University of Oxford, Oxford, UK
7. National Heart and Lung Institute, Imperial College London, London, UK
8. Imperial College Healthcare NHS Trust: London, London, UK
9. National Infection Service, Public Health England, London, UK
10. Centre for Inflammation Research, The Queen's Medical Research Institute, University of Edinburgh, Edinburgh, UK
11. Edinburgh Pathology, University of Edinburgh, Edinburgh, UK
12. Antimicrobial Resistance and Hospital Acquired Infection Department, Public Health England, London, UK
13. Blood Borne Virus Unit, Virus Reference Department, National Infection Service, Public Health England, London, UK
14. Transfusion Microbiology, National Health Service Blood and Transplant, London, UK
15. Department of Medicine, Imperial College London, London, UK
16. Department of Pharmacology, University of Liverpool, Liverpool, UK
17. Tropical & Infectious Disease Unit, Royal Liverpool University Hospital, Liverpool, UK
18. Walton Centre NHS Foundation Trust, Liverpool, UK
19. Liverpool School of Tropical Medicine, Liverpool, UK
20. MRC-University of Glasgow Centre for Virus Research, Glasgow, UK
21. Department of Infectious Diseases, Queen Elizabeth University Hospital, Glasgow, UK

22. Centre for Clinical Infection and Diagnostics Research, Department of Infectious Diseases, School of Immunology and Microbial Sciences, King's College London, London, UK
23. Department of Infectious Diseases, Guy's and St Thomas' NHS Foundation Trust, London, UK
24. Division of Infection & Immunity, University College London and Great Ormond Street Hospital, London, UK
25. The Florey Institute for Host-Pathogen Interactions, Department of Infection, Immunity and Cardiovascular Disease, University of Sheffield, Sheffield, UK
26. Liverpool Clinical Trials Centre, University of Liverpool, Liverpool, UK
27. Roslin Institute, University of Edinburgh, Edinburgh, UK
28. EPCC, University of Edinburgh, Edinburgh, UK
29. Public Health Scotland, UK
30. Edinburgh Clinical Research Facility, University of Edinburgh, Edinburgh, UK
31. Institute of Translational Medicine, University of Liverpool, Liverpool, Merseyside, UK
32. Sheffield Teaching Hospitals, Sheffield, UK
33. University of Liverpool, Liverpool, UK
34. Royal Hospital for Children and Young People, Edinburgh, UK
35. Department of Paediatric Infectious Diseases and Immunology, Royal Hospital for Children, Glasgow, UK
36. Royal Aberdeen Children's Hospital, Aberdeen, UK
37. University Hospital Wishaw, North Lanarkshire, UK
38. Crosshouse & Ayr Hospital, Kilmarnock, Scotland, UK
39. Dumfries & Galloway Royal Infirmary, Dumfries, UK

40. Borders General Hospital, Melrose, UK
41. Forth Valley Royal Hospital, Larbert, UK
42. Tayside Children's Hospital, Ninewells Hospital, NHS Tayside, Dundee, UK, Ninewells Hospital, NHS Tayside, Dundee, UK
43. Doncaster and Bassetlaw Teaching Hospitals NHS Foundation Trust, Doncaster, UK NHS Foundation Trust, Doncaster, UK
44. Burnley General Teaching Hospital, Burnley, UK
45. Hereford County Hospital, Herewford, UK
46. Leighton Hospital, Leighton, UK
47. Walsall Healthcare NHS Trust, Walsall, UK
48. Cumberland Infirmary, Cumberland, UK
49. Paediatric Liver, GI & Nutrition Centre and MowatLabs, King’s College Hospital, London, UK
50. Institute of Liver Studies, King’s College London, London, UK
51. Birmingham Women's Children's Hospital, Birmingham, UK
52. St Richards' Hospital, Chichester, UK
53. Airedale General Hospital, Keighley, UK
54. Hinchingbrooke Hospital, Huntingdon, UK
55. Darlington Memorial Hospital, Darlington, UK
56. Warrington Hospital, Kilmarnock, UK
57. Leeds Teaching Hospitals NHS Trust, Leeds, UK
58. Queens Hospital Burton, Burton-on-Trent, UK
59. Queen Margaret Hospital, Dunfermline, UK
60. Royal Victoria Infirmary, Newcastle upon Tyne, UK
61. Poole University Hospital, Dorset, UK

62. Bradford Royal infirmary, Bradford, UK
63. Department of Paediatric Gastroenterology, Hepatology and Nutrition, Royal Hospital for Children, Glasgow, UK
64. Avon and Wiltshire Mental Health Partnership NHS Trust, Bath, UK
65. Royal Hospital For Children and Young People, Edinburgh, UK
66. Queen Elizabeth University Hospital, Glasgow, UK
67. University Hospital Crosshouse, Kilmarnock, UK
68. Royal Free Hospital, London, UK
69. Diana Princess of Wales Hospital, Grimsby, UK
70. King's College Hospital, London, UK
71. Western General Hospital, Edinburgh, UK
72. Barnsley Hospital, Barnsley, UK
73. Bradford Teaching Hospitals NHS Foundation Trust, Bradford, UK
74. Wye Valley NHS Trust, Hereford, UK
75. Newcastle upon Tyne Hospitals NHS Foundation Trust, Newcastle upon Tyne, UK
76. West Cumberland Hospital, Whitehaven, UK
77. University Hospital of North Durham, Durham, UK
78. Worthing Hospital, Worthing, UK

DIAMONDS Consortium

PARTNER: Imperial College (Coordinating Centre) (UK)

Chief investigator/DIAMONDS coordinator:

Michael Levin[1]

Principal and co-investigators (alphabetical order)[1]

Aubrey Cunnington; Jethro Herberg; Myrsini Kaforou; Victoria Wright

Section of Paediatric Infectious Diseases Research Group (alphabetical order)[1]

Evangelos Bellos; Claire Broderick; Samuel Channon-Wells; Samantha Cooray; Tisham De (database work package lead); Giselle D'Souza; Leire Estramiana Elorrieta; Diego Estrada-Rivadeneyra; Rachel Galassini (Clinical Trial Manager); Dominic Habgood-Coote; Shea Hamilton (Proteomics); Heather Jackson; James Kavanagh; Mahdi Moradi Marjaneh; Stephanie Menikou; Samuel Nichols; Ruud Nijman; Harsita Patel; Ivana Pennisi; Oliver Powell; Ruth Reid; Priyen Shah; Ortensia Vito; Elizabeth Whittaker; Clare Wilson; Rebecca Womersley

Recruitment team at Imperial College Healthcare NHS Trust, London (alphabetical order)[2]

Amina Abdulla; Sarah Darnell; Sobia Mustafa

Engineering Team

Pantelis Georgiou[3] (engineering lead); Jesus-Rodriguez Manzano[4]; Nicolas Moser[3]; Ivana Pennisi[1]

1. 1.Section of Paediatric Infectious Disease, Imperial College London, Norfolk Place, London W2 1PG, UK
2. 2.Children's Clinical Research Unit, St Mary's Hospital, Praed Street, London W2 1NY, UK
3. 3.Imperial College London, Department of Electrical and Electronic Engineering, South Kensington Campus, London, SW7 2AZ, UK
4. 4.Imperial College London, Department of Infectious Disease, Section of Adult Infectious Disease, Hammersmith Campus, London, W12 0NN, UK

UK Non-Consortium Clinical Recruiting Sites

Evelina London Children's Hospital, Guy's and St Thomas' NHS Foundation Trust; King's College London [combined]

Michael Carter[1,2] (principal investigator); Shane Tibby[1,2] (co-investigator)

Recruitment team (alphabetical order): Jonathan Cohen[1]; Francesca Davis[1]; Julia Kenny[1]; Paul Wellman[1]; Marie White[1]

Laboratory team (alphabetical order): Matthew Fish[3]; Aislinn Jennings[4]; Manu Shankar-Hari[3,4]

1. Evelina London Children's Hospital, Guy's and St Thomas' NHS Foundation Trust, London, UK
2. Department of Women and Children's Health, School of Life Course Sciences, King's College London, UK
3. Department of Infectious Diseases, School of Immunology and Microbial Sciences, King's College London, London, UK
4. Department of Intensive Care Medicine, Guy's and St Thomas' NHS Foundation Trust, London, UK

University Hospitals Sussex

Katy Fidler[1] (principal investigator); Dan Agranoff[2] (co-investigator)

Recruitment team; Vivien Richmond[1,3], Mathhew Seal[2]

1. Royal Alexandra Children's Hospital, University Hospitals Sussex, Brighton, UK
2. Dept of Infectious Diseases, University Hospitals Sussex, Brighton, UK
3. Research Nurse team, University Hospitals Sussex, Brighton, UK

University Hospital Southampton NHS Foundation Trust

Saul Faust[1] (principal investigator); Dan Owen[1] (co-investigator);

Recruitment team: Ruth Ensom[2]; Sarah McKay[2]; Diana Mondo[3], Mariya Shaji[3]; Rachel Schranz[3] (alphabetical order)

1. NIHR Southampton Clinical Research Facility, University Hospital Southampton NHS Foundation Trust and University of Southampton, UK
2. NIHR Southampton Clinical Research Facility, University Hospital Southampton NHS Foundation Trust, UK
3. Department of R&D, University Hospital Southampton NHS Foundation Trust, UK

Barts Health NHS Trust

Prita Rughnani[1, 2, 3] (principal investigator 2020-2021); Amutha Anpananthar[1, 2, 3] (principal investigator 2021-to date); Susan Liebeschuetz[2] (co-investigator), Anna Riddell[1] (co-investigator)

Recruitment team; Nosheen Khalid[1,3], Ivone Lancoma Malcolm, Teresa Simagan[3] (alphabetical order)

1. Royal London Hospital, Whitechapel Rd, London E1 1FR, UK
2. Newham University Hospital, Glen Rd, London E13 8SL, UK
3. Whipps Cross University Hospital, Whipps Cross Road, London, E11 1NR, UK

Great Ormond Street Hospital for Children NHS Foundation Trust

Mark Peters[1,2] (principal investigator); Alasdair Bamford[1,2] (co-investigator)

Recruitment team; Lauran O'Neill[1]

1. Great Ormond Street Hospital, London, WC1N 3JH, UK
2. UCL Great Ormond St Institute of Child Health, WC1N 1EH, UK

Cambridge University Hospitals NHS Foundation Trust

Nazima Pathan[1,2] (principal investigator)

Recruitment team; Esther Daubney[1], Deborah White[1] (alphabetical order)

1. Addenbrooke's Hospital, Hills Road, Cambridge CB2 0QQ, UK
2. Department of Paediatrics, University of Cambridge, Cambridge CB2 0QQ, UK

University College London Hospitals NHS Foundation Trust

Melissa Heightman[1] (principal investigator); Sarah Eisen[1] (co-investigator)

Recruitment team; Terry Segal[1], Lucy Wellings[1] (alphabetical order)

1. University College London Hospital, Euston Road, London NW1 2BU, UK

St George's University Hospitals NHS Foundation Trust

Simon B Drysdale[1] (principal investigator)

Recruitment team; Nicole Branch[1], Lisa Hamzah[1], Heather Jarman[1] (alphabetical order)

1. St George's Hospital, Blackshaw Road, London SW17 0QT, UK

Lewisham and Greenwich NHS Trust

Maggie Nyirenda[1, 2,] (principal investigator)

Recruitment team Lisa Capozzi[1], Emma Gardiner[1] (alphabetical order)

1. University Hospital Lewisham, London SE13 6LH, UK
2. Queen Elizabeth Hospital Greenwich, London SE18 4QH, UK

Liverpool University Hospitals NHS Foundation Trust

Robert Moots[1] (principal investigator); Magda Nasher[2] (principal investigator)

Recruitment team; Anita Hanson[2]; Michelle Linforth[1]

1. Aintree University Hospital, Lower Lane, Liverpool L9 7AL, UK
2. Royal Liverpool Hospital, Prescot St, Liverpool L7 8XP, UK

Leeds Teaching Hospitals NHS Trust

Sean O'Riordan[1] (principal investigator)

Recruitment team; Donna Ellis[1]

1. Leeds Children's Hospital, Leeds LS1 3EX, UK

King's College Hospital NHS Foundation Trust

Akash Deep[1] (principal investigator)

Recruitment team; Ivan Caro[1]

1. Kings College Hospital, Denmark Hill, London SE5 9RS, UK

Sheffield Children's NHS Foundation Trust

Fiona Shackley[1] (principal investigator)

Recruitment team; Arianna Bellini[1] Stuart Gormley[1] (alphabetical order)

1. Sheffield Children's Hospital, Broomhall, Sheffield S10 2TH, UK

University Hospitals of Leicester NHS Foundation Trust

Samira Neshat[1] (principal investigator)

1. Leicester General Hospital, Leicester LE1 5WW, UK

Birmingham Women's and Children's Hospital NHS Foundation Trust

Barnaby J Scholefield[1] (principal investigator)

Recruitment team; Ceri Robbins[1], Helen Winmill[1] (alphabetical order)

1. Birmingham Children's Hospital, Steelhouse Lane, Birmingham B4 6NH, UK

PARTNER: University of Oxford (UK)

Children's Hospital, John Radcliffe Hospital, Oxford

Principal Investigator: Stéphane C. Paulus[1,2,3]

Co-Principal Investigator: Andrew J. Pollard[1,2,3,4]

Co-investigators: Mark Anthony[1] (neonates)

Recruitment team: Sarah Hopton[1], Danielle Miller[1], Zoe Oliver[1], Sally Beer[1], Bryony Ward[1]

1. John Radcliffe Hospital, Oxford University Hospitals NHS Foundation Trust, Oxford, UK
2. Department of Paediatrics, University of Oxford, UK
3. Oxford Vaccine Group, University of Oxford, UK
4. NIHR Oxford Biomedical Research Centre, Oxford, UK

University of Oxford, Nepal Site

Principal Investigator: Shrijana Shrestha[1]

Co-Principal Investigator: Andrew J Pollard[2,3]

Nepal Research Team: Meeru Gurung[1], Puja Amatya[1], Bhishma Pokhrel[1], Sanjeev Man Bijukchhe[1]

Oxford Research Team: Tim Lubinda[2], Sarah Kelly[2], Peter O'Reilly[2]

1. Paediatric Research Unit, Patan Academy of Health Sciences, Kathmandu, Nepal.
2. Oxford Vaccine Group, Department of Paediatrics, University of Oxford, Oxford, United Kingdom.

3. NIHR Oxford Biomedical Research Centre, Oxford, United Kingdom.

PARTNER: SERGAS (Spain)

Principal Investigators: Federico Martinón-Torres[1], Antonio Salas[1,2]

GENVIP RESEARCH GROUP (in alphabetical order):

Fernando Álvez González[1], Xabier Bello[1,2], Mirian Ben García[1], Sandra Carnota[1], Miriam Cebey-López[1], María José Curras-Tuala[1,2], Carlos Durán Suárez[1], Luisa García Vicente[1], Alberto Gómez-Carballa[1,2,] Jose Gómez Rial[1], Pilar Leboráns Iglesias[1], Federico Martinón-Torres[1], Nazareth Martinón-Torres[1], José María Martinón Sánchez[1], Belén Mosquera Pérez[1], Jacobo Pardo-Seco[1,2], Lidia Piñeiro Rodríguez[1], Sara Pischedda[1,2,] Sara Rey Vázquez[1], Irene Rivero Calle[1], Carmen Rodríguez-Tenreiro[1], Lorenzo Redondo-Collazo[1], Miguel Sadiki Ora[1], Antonio Salas[1,2,] Sonia Serén Fernández[1], Cristina Serén Trasorras[1], Marisol Vilas Iglesias[1].

1. Translational Pediatrics and Infectious Diseases, Pediatrics Department, Hospital Clínico Universitario de Santiago, Santiago de Compostela, Spain, and GENVIP Research Group (www.genvip.org), Instituto de Investigación Sanitaria de Santiago, Universidad de Santiago de Compostela, Galicia, Spain.
2. Unidade de Xenética, Departamento de Anatomía Patolóxica e Ciencias Forenses, Instituto de Ciencias Forenses, Facultade de Medicina, Universidade de Santiago de Compostela, and GenPop Research Group, Instituto de Investigaciones Sanitarias (IDIS), Hospital Clínico Universitario de Santiago, Galicia, Spain
3. Fundación Pública Galega de Medicina Xenómica, Servizo Galego de Saúde (SERGAS), Instituto de Investigaciones Sanitarias (IDIS), and Grupo de Medicina Xenómica, Centro de Investigación Biomédica en Red de Enfermedades Raras

(CIBERER), Universidade de Santiago de Compostela (USC), Santiago de Compostela, Spain

PARTNER: Liverpool (UK)

Principal Investigator: Enitan D Carrol[1,2,]

Research Group (in alphabetical order): Elizabeth Cocklin[1], Aakash Khanijau[1], Rebecca Lenihan[1], Nadia Lewis-Burke[1], Karen Newall[3], Sam Romaine[1]

1. Department of Clinical Infection, Microbiology and Immunology, University of Liverpool Institute of Infection, Veterinary and Ecological Sciences , Liverpool, England
2. Alder Hey Children's Hospital, Department of Infectious Diseases, Eaton Road, Liverpool, L12 2AP
3. Alder Hey Children's Hospital, Clinical Research Business Unit, Eaton Road, Liverpool, L12 2AP

PARTNER: NATIONAL AND KAPODISTRIAN UNIVERSITY OF ATHENS (Greece)

Principal Investigator: Maria Tsolia[1]

Co-Investigator: Irini Eleftheriou[1]

PID Unit: Nikos Spyridis[1], Maria Tambouratzi[1]

Pediatric Rheumatology Unit: Despoina Maritsi[1]

Lab: Antonios Marmarinos1, Marietta Xagorari[1]

Recruitment teams:

Adult COVID19- Infectious Diseases: Lourida Panagiota, Pefanis Aggelos[2]

Adult COVID19: Akinosoglou Karolina, Gogos Charalambos, Maragos Markos[3]

Adult Inflammatory Diseases-Oncology: Voulgarelis Michalis, Stergiou Ioanna[4]

1. 2nd Department of Pediatrics, National and Kapodistrian University of Athens (NKUA), Children's Hospital "P, and A. Kyriakou", Athens, Greece
2. 1st Department of Infectious Diseases, General Hospital "Sotiria"
3. Pathology Department, University of Patras, General Hospital "Panagia i Voithia"
4. Pathophysiology Department, Medical Faculty, National and Kapodistrian University of Athens (NKUA), General Hospital "Laiko"

Newcastle upon Tyne Hospitals NHS Foundation Trust and Newcastle University (UK) combined

Principal Investigator: Marieke Emonts [1,2,3] (all activities)

Co-investigators: Emma Lim[2,3,6] (all activities), John Isaacs[1] (adult inflammatory)

Recruitment team (alphabetical), data managers, and GNCH Research unit:

Kathryn Bell[4], Stephen Crulley[4], Daniel Fabian[4], Evelyn Thomson[4], Diane Wallia[4], Caroline Miller[4], Ashley Bell[4]

PhD Students/medical staff DIAMONDS:

Fabian J.S. van der Velden[1,2] (all activities), Geoff Shenton[7] (oncology), Ashley Price[8,9] (Adult COVID)

Students:

Owen Treloar [1,2] (quality control, data management and analysis)

Daisy Thomas[1,2] (recruitment)

1. Translational and Clinical Research Institute, Newcastle University, Newcastle upon Tyne UK
2. Great North Children's Hospital, Paediatric Immunology, Infectious Diseases & Allergy, Newcastle upon Tyne Hospitals NHS Foundation Trust, Newcastle upon Tyne, United Kingdom.

3. NIHR Newcastle Biomedical Research Centre based at Newcastle upon Tyne Hospitals NHS Trust and Newcastle University, Westgate Rd, Newcastle upon Tyne NE4 5PL, United Kingdom
4. Great North Children's Hospital, Research Unit, Newcastle upon Tyne, UK
5. Hospitals NHS Foundation Trust, Newcastle upon Tyne, United Kingdom.
6. Population Health Sciences Institute, Newcastle University, Newcastle upon Tyne, UK
7. Great North Children's Hospital, Paediatric Oncology, Newcastle upon Tyne Hospitals NHS Foundation Trust, Newcastle upon Tyne, United Kingdom.
8. Department of Infection & Tropical Medicine, Newcastle upon Tyne Hospitals NHS Foundation Trust, Newcastle upon Tyne, United Kingdom
9. NIHR Newcastle In Vitro Diagnostics Co-operative (Newcastle MIC), Newcastle upon Tyne, United Kingdom.

Servicio Madrileño de Salud (SERMAS) - Fundación Biomédica del Hospital Universitario 12 de Octubre (FIB-H12O) (Spain)

Principal Investigators: Pablo Rojo[1,3], Cristina Epalza[1,2]

SERMAS/FIB-H120 team: Serena Villaverde[1], Sonia Márquez[2], Manuel Gijón[2], Fátima Machín[2], Laura Cabello[2], Irene Hernández[2], Lourdes Gutiérrez[2], Ángela Manzanares[1]

1. Servicio Madrileño de Salud (SERMAS),Pediatric Infectious Diseases Unit, Department of Pediatrics, Hospital Universitario 12 de Octubre, Madrid, Spain
2. Fundación Biomédica del Hospital Universitario 12 de Octubre (FIB-H12O), Unidad Pediátrica de Investigación y Ensayos Clínicos (UPIC), Hospital Universitario 12 de Octubre, Instituto de Investigación Sanitaria Hospital 12 de Octubre (i+12), Madrid, Spain.

3. Universidad Complutense de Madrid, Faculty of Medicine, Department of Pediatrics, Madrid, Spain.

Amsterdam University Medical Center (Amsterdam UMC), University of Amsterdam

Principal Investigator: T.W. (Taco) Kuijpers MD PhD[1,2] (all activities)

Co-investigators: M. (Martijn) van de Kuip MD PhD[1] (infectious disease), A.M. (Marceline) van Furth MD PhD[1] (infectious disease), J.M. (Merlijn) van den Berg MD PhD[1] (inflammatory disease)

Hospital Team (all activities): Giske Biesbroek MD PhD[1], Floris Verkuil MD (PhD student) [1], Carlijn (C.W.) van der Zee MD (PhD student) [1]

Recruitment: Dasja Pajkrt MD PhD[1], Michael Boele van Hensbroek MD PhD[1], Dieneke Schonenberg MD[1], Mariken Gruppen MD[1], Sietse Nagelkerke MD PhD[1,2], medical students

Laboratory Team: Machiel H Jansen[1], Ines Goetschalckx (PhD student) [2]

1. Amsterdam UMC, Emma Children's Hospital, Dept of Pediatric Immunology, Rheumatology and Infectious Disease, University of Amsterdam, The Netherlands
2. Sanquin, Dept of Molecular Hematology, University Medical Center, Amsterdam, The Netherlands

Bambino Gesù Children’s Hospital (Rome-Italy)

Principal Investigators: Lorenza Romani[1] , Maia De Luca[1]

Recruitment Team: Sara Chiurchiù[1], Martina Di Giuseppe[1]

1. Infectious Disease Unit, Academic Department of Pediatrics, Bambino Gesù Children's Hospital, IRCCS, Rome 00165, Italy

ERASMUS MC-Sophia Children's Hospital

Principal Investigator: Clementien L. Vermont[2]

Research group: Henriëtte A. Moll[1], Dorine M. Borensztajn[1], Nienke N. Hagedoorn, Chantal Tan [1], Joany Zachariasse [1], Medical students [1]

Additional investigator: W Dik[3]

1. Erasmus MC-Sophia Children's Hospital, Department of General Paediatrics, Rotterdam, the Netherlands
2. Erasmus MC-Sophia Children's Hospital, Department of Paediatric Infectious Diseases & Immunology, Rotterdam, the Netherlands
3. Erasmus MC, Department of immunology, Rotterdam, the Netherlands

TAIWAN

Ching-Fen (Kitty), Shen

Division of Infectious Disease, Department of Pediatrics, National Cheng Kung University Tainan, Taiwan

Riga Stradins University (Riga, Latvia)

Principal Investigator: Dace Zavadska[1,2] (all activities)

Co-investigators: Sniedze Laivacuma[1,3] (adult cohorts)

Recruitment team: Aleksandra Rudzate[1,2], Diana Stoldere[1,2], Arta Barzdina[1,2], Elza Barzdina[1,2], Sniedze Laivacuma[1,3], Monta Madelane[1,3]

Laboratory: Dagne Gravele[2], Dace Svile[2]

1. Riga Stradins University, Riga, Latvia
2. Children clinical university hospital, Riga, Latvia
3. Riga East clinical university hospital, Riga, Latvia

Assistance Publique - Hôpitaux de Paris

Principal Investigator: Romain Basmaci[1,2]

Co-investigator: Noémie Lachaume[1]

Recruitment team: Pauline Bories[1], Raja Ben Tkhayat[1], Laura Chériaux[1], Juraté Davoust[1], Kim-Thanh Ong[1], Marie Cotillon[1], Thibault de Groc[1], Sébastien Le[1], Nathalie Vergnault[1], Hélène Sée[1], Laure Cohen[1], Alice de Tugny[1], Nevena Danekova[1]

1. Service de Pédiatrie-Urgences, AP-HP, Hôpital Louis-Mourier, F-92700 Colombes, France
2. Université Paris Cité, Inserm, IAME, F-75018 Paris, France

BioMérieux

Principal Investigator: Marine Mommert-Tripon

Co-investigator: Karen Brengel-Pesce

Author Affiliations:

bioMérieux - Open Innovation & Partnerships Department, Lyon, France

University Medical Centre Ljubljana, Slovenia

Principal Investigator: Marko Pokorn[1,2,3]

Co-Investigator: Mojca Kolnik[2]

Research Group (in alphabetical order): Tadej Avčin[2,3], Tanja Avramoska[2], Natalija Bahovec[1], Petra Bogovič[1], Lidija Kitanovski[2,3], Mirijam Nahtigal[1], Lea Papst[1], Tina Plankar Srovin[1], Franc Strle[1,2], Anja Srpčič[2], Katarina Vincek[1]

1. Department of Infectious diseases, University Medical Centre Ljubljana, Slovenia
2. University Children's Hospital, University Medical Centre Ljubljana, Slovenia
3. Faculty of Medicine, University of Ljubljana, Slovenia

4. Centre for Clinical research, University Medical Centre Ljubljana

University Medical Center Utrecht, Utrecht, The Netherlands

Principal Investigator: Michiel van der Flier[1,5] (Pediatric Infectious Diseases and Immunology)

Co-investigators: Wim J.E. Tissing[5] (Pediatric Oncology), Roelie M. Wösten-van Asperen[2] (Pediatric Intensive Care Unit), Sebastiaan J Vastert[3] (Pediatric Rheumatology), Daniel C Vijlbrief[4] (Pediatric Neonatal Intensive Care), Louis J. Bont[1,5] (Pediatric Infectious Diseases and Immunology), Tom F.W. Wolfs[1,5] (Pediatric Infectious Diseases and Immunology)

PhD student: Coco R. Beudeker[1,5] (Pediatric Infectious Diseases and Immunology)

1. Pediatric Infectious Diseases and Immunology
2. Pediatric Intensive Care Unit
3. Pediatric Rheumatology
4. Pediatric Neonatal Intensive Care, Wilhelmina Children's Hospital, University Medical Center Utrecht, Utrecht, The Netherlands
5. Princess Maxima Center for Pediatric Oncology, Utrecht, The Netherlands

PARTNER: University of Bern, Inselspital, Bern University Hospital, University of Bern (Switzerland)

Principal Investigators (alphabetical): Philipp Agyeman[1], Luregn Schlapbach[2,3]

Co-Investigator: Christoph Aebi[1]

Recruitment team: Mariama Usman[1], Stefanie Schlüchter[1], Verena Wyss[1], Nina Schöbi[1], Elisa Zimmermann[2] PhD, Marion Meier[2], Kathrin Weber[2]

1. Department of Pediatrics, Inselspital, Bern University Hospital, University of Bern, Switzerland

2. Department of Intensive Care and Neonatology, and Children`s Research Center, University Children`s Hospital Zurich, Zurich, Switzerland
3. Child Health Research Centre, The University of Queensland, Brisbane, Australia

Swiss Pediatric Sepsis Study group

Philipp Agyeman, MD[1], Luregn J Schlapbach MD, FCICM[2,3], Eric Giannoni, MD[4,5], Martin Stocker, MD[6], Klara M Posfay-Barbe, MD[7], Ulrich Heininger, MD[8], Sara Bernhard-Stirnemann, MD[9], Anita Niederer-Loher, MD[10], Christian Kahlert, MD[10], Giancarlo Natalucci, MD[11], Christa Relly, MD[12], Thomas Riedel, MD[13], Christoph Aebi, MD[1], Christoph Berger, MD[12]

1. Department of Pediatrics, Inselspital, Bern University Hospital, University of Bern, Switzerland
2. Department of Intensive Care and Neonatology, and Children`s Research Center, University Children`s Hospital Zurich, Zurich, Switzerland
3. Child Health Research Centre, The University of Queensland, Brisbane, Australia
4. Clinic of Neonatology, Department Mother-Woman-Child, Lausanne University Hospital and University of Lausanne, Switzerland
5. Infectious Diseases Service, Department of Medicine, Lausanne University Hospital and University of Lausanne, Switzerland
6. Department of Pediatrics, Children's Hospital Lucerne, Lucerne, Switzerland
7. Pediatric Infectious Diseases Unit, Children's Hospital of Geneva, University Hospitals of Geneva, Geneva, Switzerland
8. Infectious Diseases and Vaccinology, University of Basel Children's Hospital, Basel, Switzerland
9. Children's Hospital Aarau, Aarau, Switzerland

10. Division of Infectious Diseases and Hospital Epidemiology, Children's Hospital of Eastern Switzerland St. Gallen, St. Gallen, Switzerland
11. Department of Neonatology, University Hospital Zurich, Zurich, Switzerland
12. Division of Infectious Diseases and Hospital Epidemiology, and Children's Research Center, University Children's Hospital Zurich, Switzerland
13. Children's Hospital Chur, Chur, Switzerland

Micropathology Ltd (UK)

Micropathology Ltd, The Venture Center, University of Warwick Science Park, Sir William Lyons Road, Coventry, CV4 7EZ
Principle Investigator; Prof Colin Fink
Co Investigators: Marie Voice, Leo Calvo-Bado, Michael Steele, Jennifer Holden
Research group: Benjamin Evans, Jake Stevens, Peter Matthews, Kyle Billing

Medical University of Graz, Austria (MUG)

Principal Investigator: Werner Zenz1 (all activities)
Co-investigators (in alphabetical order): Alexander Binder[1] (grant application), Benno Kohlmaier[1] (study design, recruitment), Daniela S. Kohlfürst[1] (study design), Nina A. Schweintzger[1] (all activities), Christoph Zurl[1] (study design, recruitment)
Recruitment team, data managers, laboratory work (in alphabetical order): Susanne Hösele[1], Manuel Leitner[1], Lena Pölz[1], Alexandra Rusu[1], Glorija Rajic[1], Bianca Stoiser[1], Martina Strempfl[1], Manfred G. Sagmeister[1]
Clinical recruitment partners (in alphabetical order):
Sebastian Bauchinger[1], Martin Benesch[3], Astrid Ceolotto[1], Ernst Eber[2], Siegfried Gallistl[1], Harald Haidl[1], Almuthe Hauer[1], Christa Hude[1], Andreas Kapper[7], Markus Keldorfer[5], Sabine

Löffler[5], Tobias Niedrist[6], Heidemarie Pilch[5], Andreas Pfleger[2], Klaus Pfurtscheller[4], Siegfried Rödl[4], Andrea Skrabl-Baumgartner[1], Volker Strenger[3], Elmar Wallner[7]

1. Department of Pediatrics and Adolescent Medicine, Division of General Pediatrics, Medical University of Graz, Graz, Austria
2. Department of Pediatric Pulmonology, Medical University of Graz, Graz, Austria
3. Department of Pediatric Hematooncology, Medical University of Graz, Graz, Austria
4. Paediatric Intensive Care Unit, Medical University of Graz, Graz, Austria
5. University Clinic of Pediatrics and Adolescent Medicine Graz, Medical University Graz, Graz, Austria
6. Clinical Institute of Medical and Chemical Laboratory Diagnostics, Medical University Graz, Graz, Austria
7. Department of Internal Medicine, State Hospital Graz II, Location West, Graz, Austria

SkylineDX

Principle investigator: Dennie Tempel[1]

Co-investigators: Danielle van Keulen[1], Annelieke M Strijbosch[1],

1. SkylineDx, Rotterdam, The Netherlands

Project partner BBMRI-ERIC

Maike K. Tauchert

Biobanking and BioMolecular Resources Research Infrastructure - European Research Infrastructure Consortium (BBMRI-ERIC), Neue Stiftingtalstrasse 2/B/6, 8010, Graz, Austria

LMU Munich Partner (Germany)

Principal Investigator: Ulrich von Both[1,2] MD, FRCPCH (all activities)

Research group: Laura Kolberg[1] MSc (all activities), Patricia Schmied[1] (Study physician), Irene Alba-Alejandre[3] MD (Study physician)

Clinical recruitment partners (in alphabetical order): Katharina Danhauser, MD[6], Nikolaus Haas, MD[11], Florian Hoffmann, MD[10], Matthias Griese, MD[7], Tobias Feuchtinger, MD[5], Sabrina Juranek, MD[4], Matthias Kappler, MD[7], Eberhard Lurz, MD[8], Esther Maier, MD[4], Karl Reiter, MD[10], Carola Schoen, MD[10], Sebastian Schroepf, MD[9]

1. Division of Pediatric Infectious Diseases, Department of Pediatrics, Dr. von Hauner Children's Hospital, University Hospital, LMU Munich, Munich, Germany
2. German Center for Infection Research (DZIF), Partner Site Munich, Munich, Germany
3. Department of Gynecology and Obstetrics, University Hospital, LMU Munich, Munich, Germany
4. Division of General Pediatrics, Department of Pediatrics, Dr. von Hauner Children's Hospital, University Hospital, LMU Munich, Munich, Germany
5. Division of Pediatric Haematology & Oncology, Department of Pediatrics, Dr. von Hauner Children's Hospital, University Hospital, LMU Munich, Munich, Germany
6. Division of Pediatric Rheumatology, Department of Pediatrics, Dr. von Hauner Children's Hospital, University Hospital, LMU Munich, Munich, Germany
7. Division of Pediatric Pulmonology, Department of Pediatrics, Dr. von Hauner Children's Hospital, University Hospital, LMU Munich, Munich, Germany
8. Division of Pediatric Gastroenterology, Department of Pediatrics, Dr. von Hauner Children's Hospital, University Hospital, LMU Munich, Munich, Germany
9. Neonatal Intensive Care Unit, Department of Pediatrics, Dr. von Hauner Children's Hospital, University Hospital, LMU Munich, Munich, Germany

10. Paediatric Intensive Care Unit, Department of Pediatrics, Dr. von Hauner Children's Hospital, University Hospital, LMU Munich, Munich, Germany
11. Department of Pediatric Cardiology and Pediatric Intensive Care, University Hospital, LMU Munich, Germany

London School of Hygiene and Tropical Medicine (LSHTM)
Principal Investigator: Shunmay Yeung [1,2,3]
Research group: Manuel Dewez[1], David Bath[3], Elizabeth Fitchett[1], Fiona Cresswell[1]
1. Clinical Research Department, Faculty of Infectious and Tropical Disease, London School of Hygiene and Tropical Medicine, London
2. Department of Paediatrics, St. Mary's Imperial College Hospital, London
Department of Global Health and Development, Faculty of Public Health and Policy, London School of Hygiene and Tropical Medicine, London

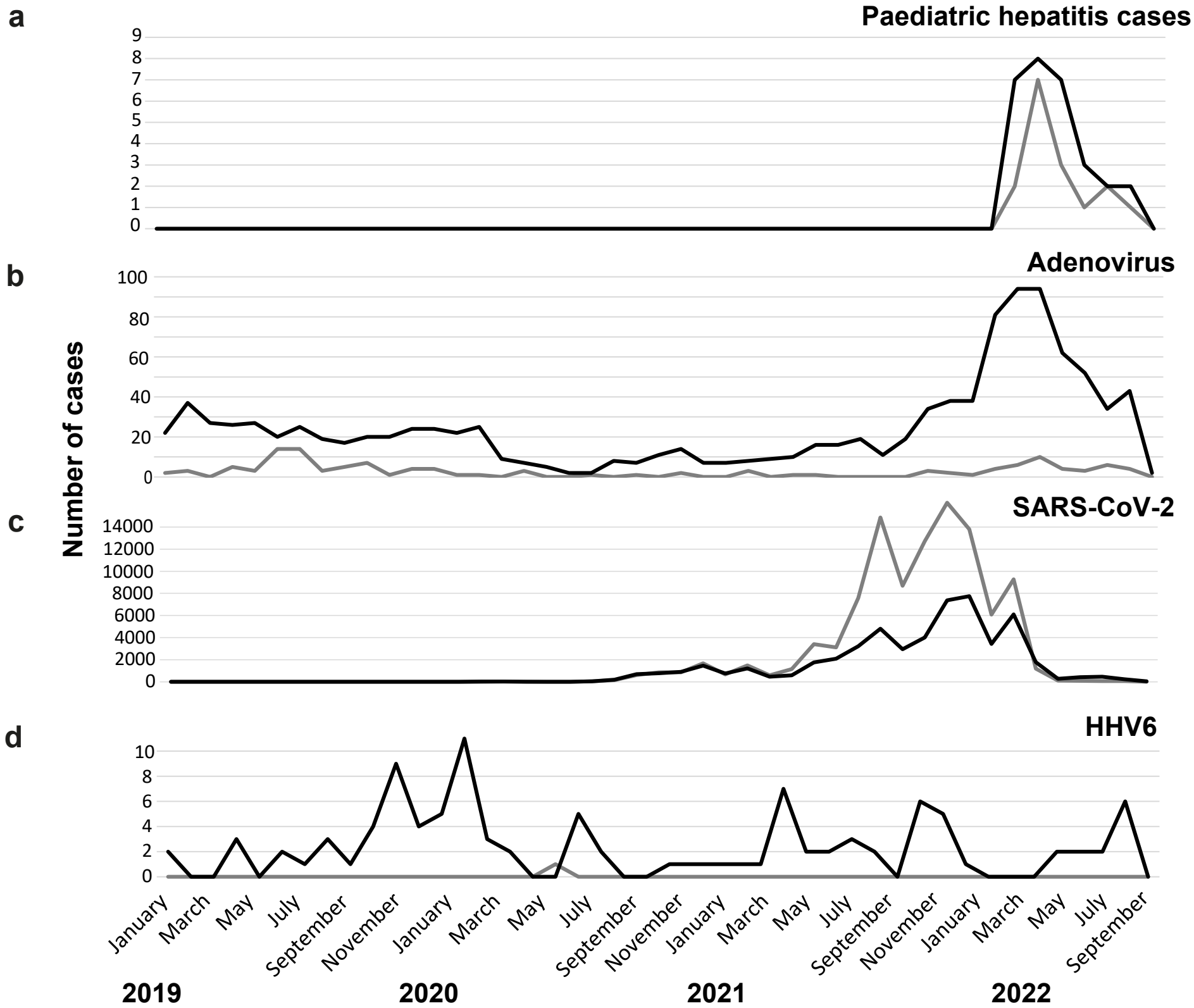
a
Paediatric hepatitis cases
9
8
7
6
5
4
3
2
1
0
b
Adenovirus
100
80
60
40
20
0
Number of cases
c
SARS-CoV-2
14000
12000
10000
8000
6000
4000
2000
0
d
HHV6
10
8
6
4
2
0
January
March
May
July
September
November
January
March
May
July
September
November
January
March
May
July
September
November
January
March
May
July
September
2019
2020
2021
2022

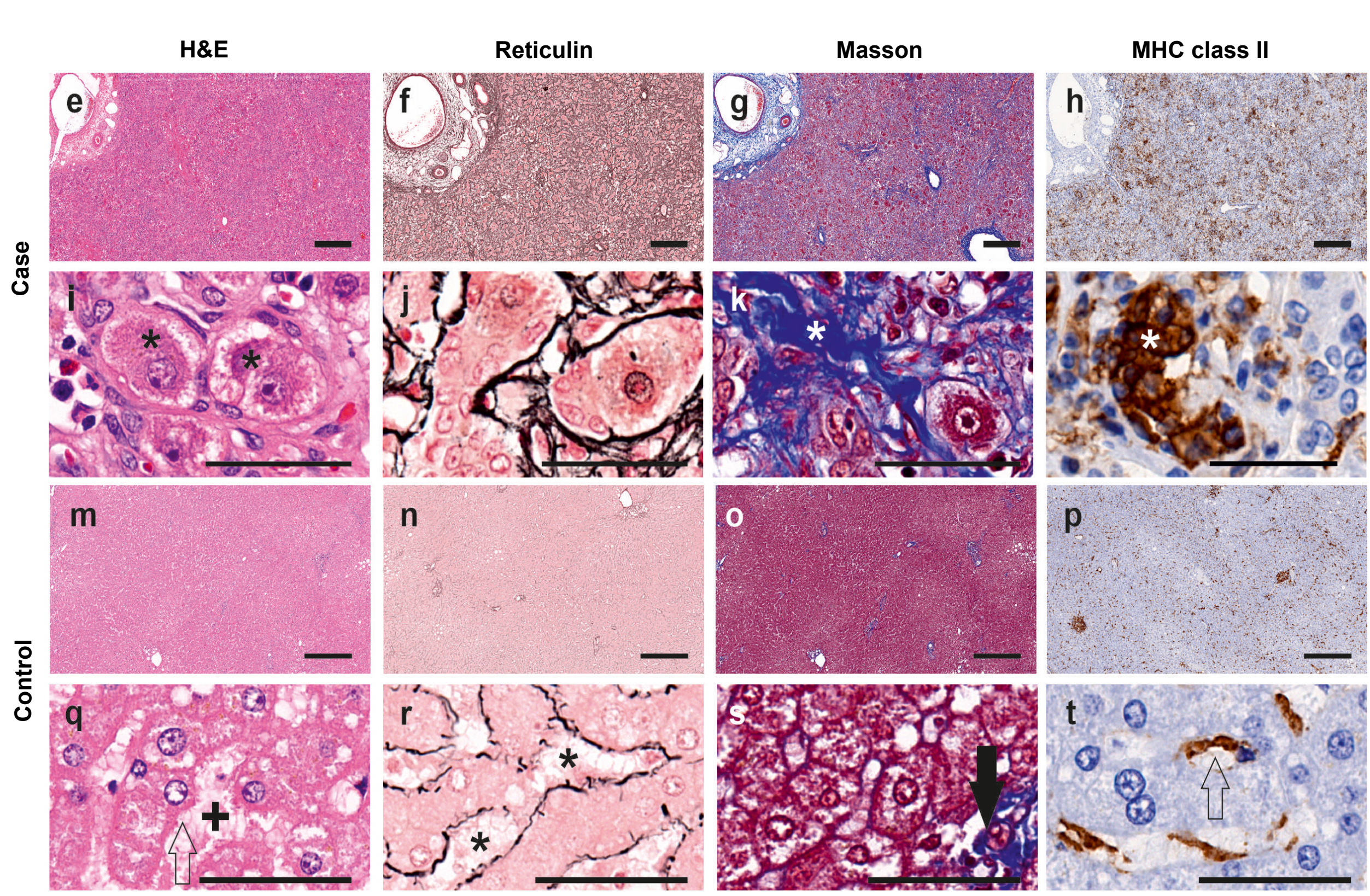
H&E
Reticulin
Masson
MHC class II
Case
Control
e
f
g
h
i
j
k
l
m
n
o
p
q
r
s
t

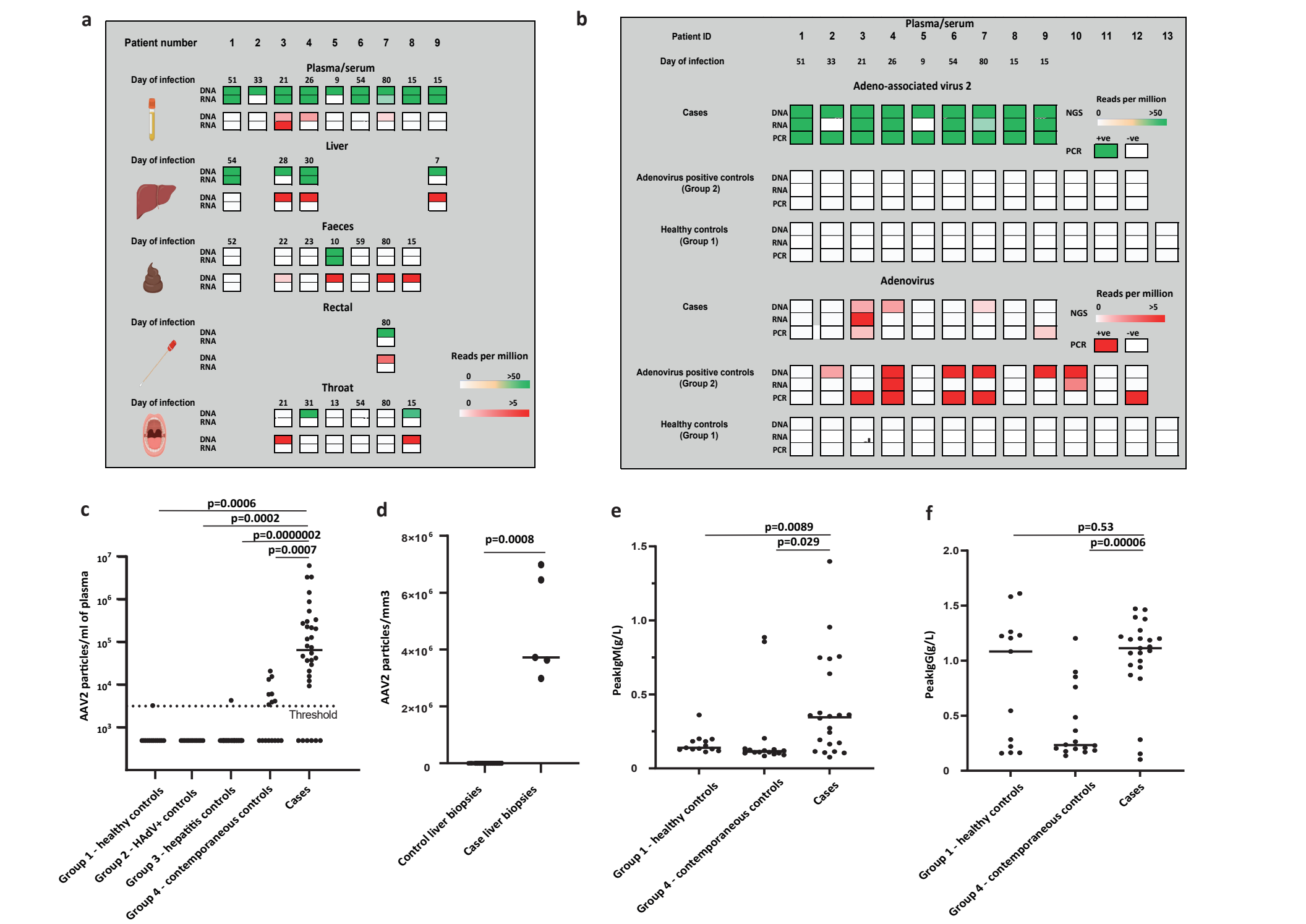
a
Patient number 1 2 3 4 5 6 7 8 9
Plasma/serum
Day of infection 51 33 21 26 9 54 80 15 15
DNA RNA
DNA RNA
Liver
Day of infection 54 28 30 7
DNA RNA
DNA RNA
Faeces
Day of infection 52 22 23 10 59 80 15
DNA RNA
DNA RNA
Rectal
Day of infection 80
DNA RNA
DNA RNA
Throat
Day of infection 21 31 13 54 80 15
DNA RNA
DNA RNA
Reads per million
0 >50
0 >5
b
Patient ID 1 2 3 4 5 6 7 8 9 10 11 12 13
Plasma/serum
Day of infection 51 33 21 26 9 54 80 15 15
Adeno-associated virus 2
Cases
DNA RNA PCR
Reads per million
NGS 0 >50
PCR +ve -ve
Adenovirus positive controls (Group 2)
DNA RNA PCR
Healthy controls (Group 1)
DNA RNA PCR
Adenovirus
Cases
DNA RNA PCR
Reads per million
NGS 0 >5
PCR +ve -ve
Adenovirus positive controls (Group 2)
DNA RNA PCR
Healthy controls (Group 1)
DNA RNA PCR
c
p=0.0006
p=0.0002
p=0.0000002
p=0.0007
AAV2 particles/ml of plasma
Threshold
Group 1 - healthy controls
Group 2 - HAdV+ controls
Group 3 - hepatitis controls
Group 4 - contemporaneous controls
Cases
d
p=0.0008
AAV2 particles/mm3
Control liver biopsies
Case liver biopsies
e
p=0.0089
p=0.029
PeakIgM(g/L)
Group 1 - healthy controls
Group 4 - contemporaneous controls
Cases
f
p=0.53
p=0.00006
PeakIgG(g/L)
Group 1 - healthy controls
Group 4 - contemporaneous controls
Cases

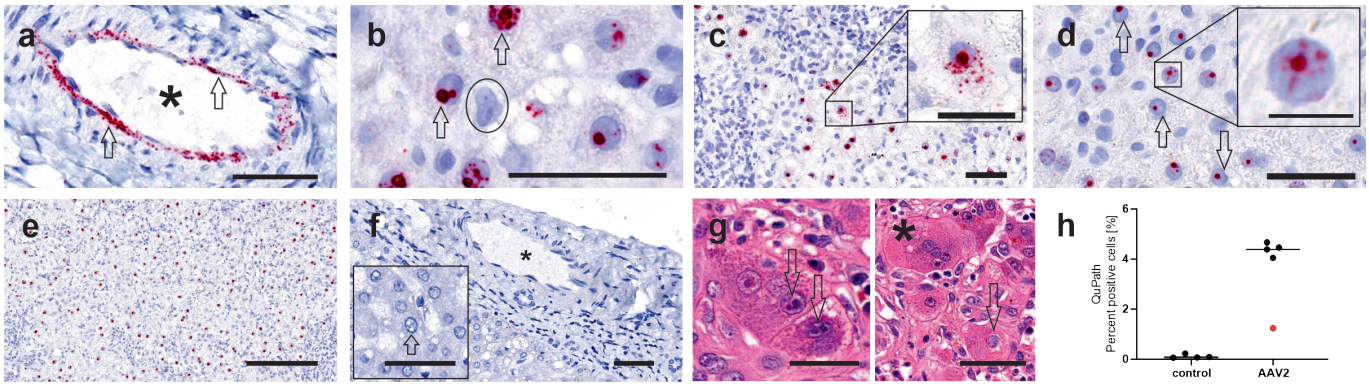
a
b
c
d
e
f
g
h
QuPath
Percent positive cells [%]
0
2
4
6
control
AAV2

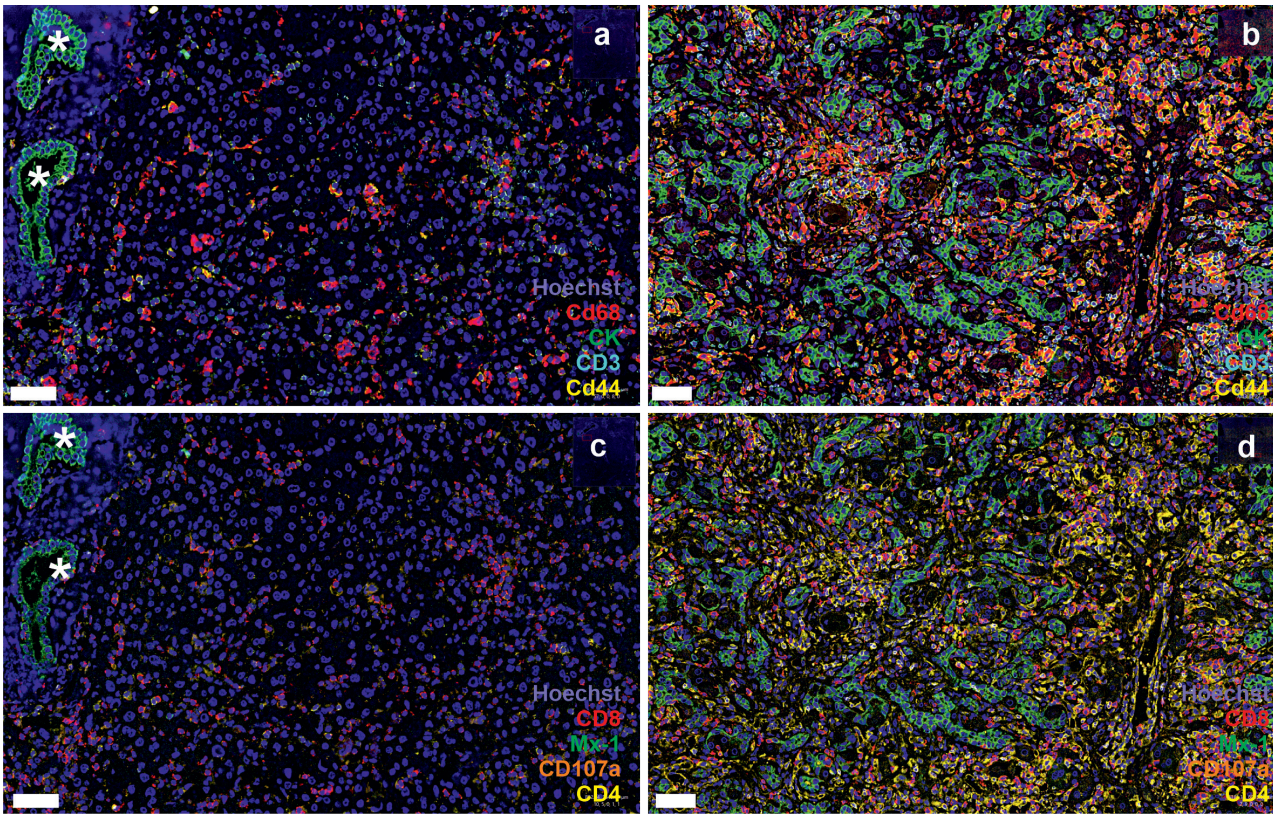
a
Hoechst
Cd68
CK
CD3
Cd44
b
Hoechst
Cd68
CK
CD3
Cd44
c
Hoechst
CD8
Mx-1
CD107a
CD4
d
Hoechst
CD8
Mx-1
CD107a
CD4